Recognition of Bipyridinium-Based Derivatives by Hydroquinone- and/or Dioxynaphthalene-Based Macrocyclic Polyethers: From Inclusion Complexes to the Self-Assembly of [2]Catenanes†

Masumi Asakawa,‡ Peter R. Ashton,‡ Sue E. Boyd,‡ Christopher L. Brown,‡ Richard E. Gillard,‡ Oldrich Kocian,‡ Françisco M. Raymo,‡ J. Fraser Stoddart,*,‡ Malcolm S. Tolley,‡ Andrew J. P. White,§ and David J. Williams§

The School of Chemistry, The University of Birmingham, Edgbaston, Birmingham B15 2TT, U.K., and Department of Chemistry, Imperial College, London SW7 2AY, U.K.

Received May 31, 1996⊗

A range of π-electron-rich macrocyclic polyethers incorporating dioxybenzene (hydroquinone) and/or dioxynaphthalene units have been synthesized in good yields by simple two-step procedures. These macrocycles are able to bind bipyridinium-based guests as a result of a series of cooperative noncovalent bonding interactions. These molecular recognition events can be extended to the self-assembly of [2]catenanes incorporating the bipyridinium-based cyclophane, cyclobis(paraquat-*p*-phenylene), and the macrocyclic polyethers incorporating dioxybenzene and -naphthalene units. The efficiencies of these self-assembly processes were found to depend upon the stereoelectronic features of the π-electron-rich macrocycles—namely, the nature and the substitution pattern of the aromatic units. X-ray crystallographic analysis of some of these [2]catenanes proved unequivocally the relative geometries of the interlocked components. In addition, in the case of those asymmetric [2]catenanes incorporating two different aromatic units within their macrocyclic polyether components, only one of the expected two translational isomers was observed in the solid state. In particular, in all the structures examined, the 1,4-dioxybenzene and 1,5-dioxynaphthalene units are located within the cavity of the tetracationic cyclophane component in preference to other regioisomeric dioxynaphthalene units that reside alongside. Variable-temperature ^{1}H NMR spectroscopic investigation of the geometries adopted by these [2]catenanes in solution revealed the same selectivity that was observed for one translational isomer over another in the solid state.

Introduction

Self-assembly[1] processes rely upon the mutual recognition of highly complementary simple molecular components whose stereoelectronic properties are responsible for the precise and efficient construction of the final thermodynamically- or kinetically-stable assemblies as a result of a series of cooperative covalent and noncovalent bonding interactions. Recently, we have developed[2] self-assembling approaches to mechanically-interlocked molecular compounds, such as catenanes and rotaxanes.[3] The methodology relies upon the complementarity between π-electron-rich hydroquinone- and/or 1,5-dioxynaphthalene-based polyethers and π-electron-deficient bipyridinium-based components. Noncovalent bonding interactions, such as (i) π−π stacking[4] between the complementary aromatic units, (ii) hydrogen bonding[5] between the polyether oxygen atoms and the acidic protons on the bipyridinium units, as well as, in some instances, (iii) edge-to-face T-type interactions[6] are mainly

Scheme 1

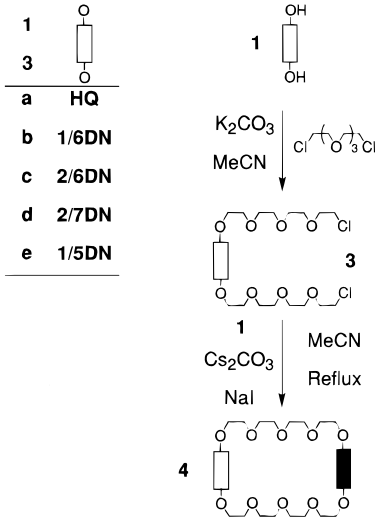

† Molecular Meccano. 11. Part 10: Anelli, P. L.; Asakawa, M.; Ashton, P. R.; Bissell, R. A.; Clavier, G.; Górski, R.; Kaifer, A. E.; Langford, S. J.; Mattersteig, G.; Menzer, S.; Philp, D.; Slawin, A. M. Z.; Spencer, N.; Stoddart, J.F.; Tolley, M. S.; Williams, D. J. *Chem. Eur. J.*, submitted.

‡ University of Birmingham.

§ Imperial College.

⊗ Abstract published in *Advance ACS Abstracts,* December 15, 1996.

(1) (a) Lindsey, J. S. *New J. Chem.* **1991**, *15*, 153−180. (b) Whitesides, G. M.; Mathias, J. P.; Seto, C. T. *Science* **1991**, *254*, 1312−1319. (c) Lawrence, D. S.; Jiang, T.; Levett, M. *Chem. Rev.* **1995**, *95*, 2229−2260. (d) Raymo, F. M.; Stoddart, J. F. *Curr. Opin. Colloid Interface Sci.* **1996**, *1*, 116−126. (e) Philp, D.; Stoddart J. F. *Angew. Chem., Int. Ed. Engl.* **1996**, *35*, 1154−1196.

(2) (a) Philp, D.; Stoddart, J. F. *Synlett* **1991**, 445−458. (b) Pasini, D.; Raymo, F. M.; Stoddart, J. F. *Gazz. Chim. Ital.* **1995**, *125*, 431−443. (c) Amabilino, D. B.; Raymo, F. M.; Stoddart, J. F. In *Comprehensive Supramolecular Chemistry*; Hosseini, M. W., Sauvage, J.-P., Eds.; 1996; pp 85−130.

(3) (a) Dietrich-Buchecker, C. O.; Sauvage J.-P. *Bioorg. Chem. Front.* **1991**, *2*, 195−248. (b) Gibson, H. W.; Marand, H. *Adv. Mater.* **1993**, *5*, 11−21. (c) Chambron, J.-C.; Dietrich-Buchecker, C. O.; Sauvage, J.-P. *Top. Curr. Chem.* **1993**, *165*, 131−162. (d) Gibson, H. W.; Bheda, M. C.; Engen., P. T. *Prog. Polym. Sci.* **1994**, *19*, 843−945. (e) Amabilino, D. B.; Stoddart, J. F. *Chem. Rev.* **1995**, *95*, 2725−2828. (f) Bělohradský, M.; Raymo, F. M.; Stoddart, J. F. *Collect. Czech. Chem. Commun.* **1996**, *61*, 1−43.

(4) (a) Foster, R. *Organic Charge-Transfer Complexes*; Academic Press: New York, 1969. (b) Schwartz, M. H. *J. Inclusion Phenom.* **1990**, *9*, 1−35. (c) Schneider, H. J. *Angew. Chem., Int. Ed. Engl.* **1991**, *30*, 1417−1436. (d) Williams, J. H. *Acc. Chem. Res.* **1993**, *26*, 593−598. (e) Hunter, C. A. *Angew. Chem., Int. Ed. Engl.* **1993**, *32*, 1584−1586. (f) Hunter, C. A. *J. Mol. Biol.* **1993**, *230*, 1025−1054. (g) Dahl, T. *Acta Chem. Scand.* **1994**, *48*, 95−116. (h) Cozzi, F.; Siegel, J. S. *Pure Appl. Chem.* **1995**, *67*, 683−689.

S0022-3263(96)01025-0 CCC: $14.00

Scheme 2

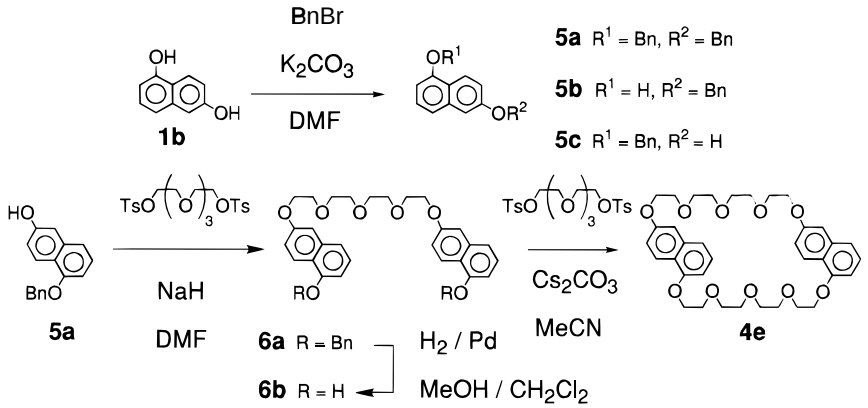

responsible for the self-assembly of these molecular compounds. Furthermore, these noncovalent bonding interactions live on in the assembled catenane or rotaxane, governing their properties both in solution and in the solid state.[7] In order to gain further insights into the operation of these self-assembly processes, we decided to introduce structural changes into the π-electron-rich components of a series of [2]catenanes. In particular, the nature of the aromatic units and their substitution patterns have been varied in order to probe the influence of stereoelectronic effects in these [2]catenanes. The effect of very subtle changes upon the molecular recognition events are often reflected in the efficiencies of the self-assembly processes, as well as in the properties of the resulting [2]catenanes.

Results and Discussion

Synthesis. The π-electron-rich macrocyclic polyethers **4a**−**d** and **4f**−**k** incorporating hydroquinone and/or dioxynaphthalene aromatic units[8] were prepared (Scheme 1) as a result of two-step synthetic procedures, in yields ranging from 15 to 27%. Alkylation of hydroquinone **1a** and of the naphthalene-based diols **1b**−**d** with an excess of tetraethylene glycol dichloride was carried out in MeCN in the presence of K_2CO_3 as a base. The excess of tetraethylene glycol dichloride was easily removed by distillation under reduced pressure to yield the dichlorides **3a**−**d** in yields ranging from 81 to 88%. The subsequent macrocyclizations were carried out under high dilution conditions by adding simultaneously separate MeCN solutions of the dichlorides **3a**−**d** and of the diols **1a**−**e** to a mixture of Cs_2CO_3 and NaI in MeCN heated at reflux. The corresponding macrocyclic polyethers **4a**−**d** and **4f**−**k** were isolated in yields ranging from 15 to 27% after column chromatography. Thus, the preparation of symmetric and asymmetric macrocyclic polyethers can be achieved in reasonable yields by employing two-step synthetic procedures that are certainly viable alternatives to the known literature procedures.[7]

In order to synthesize the macrocyclic polyether **4e** (Scheme 2) incorporating two 1,6-dioxynaphthalene rings, the protection of one of the two hydroxy groups of the starting compound **1b** is required. The monoprotected derivatives **5b,c** were prepared along with the diprotected compound **5a** by alkylation of **1b** with benzyl bromide in the presence of K_2CO_3 in DMF. Column chromatography of the crude reaction mixture gave **5a**−**c** in yields of 33, 3, and 17%, respectively, along with an unresolved mixture of **5b** and **5c** (19%). Alkylation of **5c** with tetraethylene glycol bistosylate in the presence of NaH in DMF afforded **6a** in a yield of 57%. Hydrogenolysis of **6a** gave **6b**, which was employed in the final macrocyclization with tetraethylene glycol bistosylate in the presence of Cs_2CO_3 in MeCN to afford the macrocyclic polyether **4e** in a yield of 24%.

The [2]catenanes **9a**−**k**·4PF_6 were prepared (Scheme 3) either (method A) at ambient temperature and pressure or (method B) by employing ultrahigh-pressure conditions at 40 °C. However, in all instances, 1, 2, and 2.5 molar equiv of the macrocyclic polyether **4a**−**k**, the bis(hexafluorophosphate) salt **8**·2PF_6, and 1,4-bis(bromomethyl)benzene, respectively, were employed using DMF as the solvent. The crude reaction mixtures were purified consecutively by column chromatography on silica gel and, after counterion exchange (NH_4PF_6/H_2O), by crystallization (MeCN/*i*-Pr_2O) to afford the corresponding

(5) (a) Etter, M. *Acc. Chem. Res.* **1990**, *23*, 120−126. (b) Etter, M. C.; MacDonald, J. C.; Bernstein, J. *Acta Crystallogr.* **1990**, *B46*, 256−262. (c) Desiraju, G. R. *Acc. Chem. Res.* **1991**, *24*, 290−296. (d) Aakeröy, C. B.; Seddon, K. R. *Chem. Soc. Rev.* **1993**, *22*, 397−407. (e) MacDonald, J. C.; Whitesides, G. M. *Chem. Rev.* **1994**, *94*, 2383−2420. (f) Lehn, J. M. *Pure Appl. Chem.* **1994**, *66*, 1961−1966. (g) Bernstein, J.; Davis, R. E.; Shimoni, L.; Chang, N. L. *Angew. Chem., Int. Ed. Engl.* **1995**, *34*, 1555−1573. (h) Burrows, A. D.; Chan, C. W.; Chowdhry, M. M.; McGrady, J. E.; Mingos, D. M. P. *Chem. Soc. Rev.* **1995**, *24*, 329−339.

(6) (a) Nishio, M.; Hirota, M. *Tetrahedron* **1989**, *45*, 7201−7245. (b) Oki, M. *Acc. Chem. Res.* **1990**, *23*, 351−356. (c) Jorgensen, W. L.; Severance, D. L. *J. Am. Chem. Soc.* **1990**, *112*, 4768−4774. (d) Etter, M. C. *J. Phys. Chem.* **1991**, *95*, 4601−4610. (e) Zaworotko, M. J. *Chem. Soc. Rev.* **1994**, *23*, 283−288. (f) Paliwal, S.; Geib, S.; Wilcox, C. S. *J. Am. Chem. Soc.* **1994**, *116*, 4497−4498. (g) Nishio, M.; Umezawa, Y.; Hirota, M.; Takeuchi, Y. *Tetrahedron* **1995**, *51*, 8665−8701.

(7) (a) Anelli, P. L.; Ashton, P. R.; Ballardini, R.; Balzani, V.; Delgado, M.; Gandolfi, M. T.; Goodnow, T. T.; Kaifer, A. E.; Philp, D.; Pietraszkiewicz, M.; Prodi, L.; Reddington, M. V.; Slawin, A. M. Z.; Spencer, N.; Stoddart, J. F.; Vicent, C.; Williams, D. J. *J. Am. Chem. Soc.* **1992**, *114*, 193−218. (b) Amabilino, D. B.; Ashton, P. R.; Brown, C. L.; Córdova, E.; Godínez, L. A.; Goodnow, T. T.; Kaifer, A. E.; Newton, S. P.; Pietraszkiewicz, M.; Philp, D.; Raymo, F. M.; Reder, A. S.; Rutland, M. T.; Slawin, A. M. Z.; Spencer, N.; Stoddart, J. F.; Williams, D. J. *J. Am. Chem. Soc.* **1995**, *117*, 1271−1293. (c) Amabilino, D. B.; Anelli, P. L.; Ashton, P. R.; Brown, G. R.; Córdova, E.; Godínez, L. A.; Hayes, W.; Kaifer, A. E.; Philp, D.; Slawin, A. M. Z., Spencer, N.; Stoddart, J. F.; Tolley, M. S.; Williams, D. J. *J. Am. Chem. Soc.* **1995**, *117*, 11142−11170. (d) Ashton, P. R.; Ballardini, R.; Balzani, V.; Credi, A.; Gandolfi, M. T.; Menzer, S.; Pérez-García, L.; Prodi, L.; Stoddart, J. F.; Venturi, M.; White, A. J. P.; Williams, D. J. *J. Am. Chem. Soc.* **1995**, *117*, 11171−11197. (e) Ashton, P. R.; Huff, J.; Menzer, S.; Parsons, I. W.; Preece, J.A.; Stoddart, J. F.; Tolley, M. S.; White, A. J. P.; Williams, D J. *Chem. Eur. J.* **1996**, *2*, 31−44. (f) Asakawa, M.; Ashton, P. R.; Menzer, S.; Raymo, F. M.; Stoddart, J. F.; White, A. J. P.; Williams, D J. *Chem. Eur. J.* **1996**, 877−893.

(8) In order to indicate the nature of the aromatic units incorporated within the π-electron-rich polyethers shown in the figures and schemes, the acronyms HQ and *n*/*m*DN, standing for hydroquinone and *n*,*m*-dioxynaphthalene, respectively, are employed.

Scheme 3

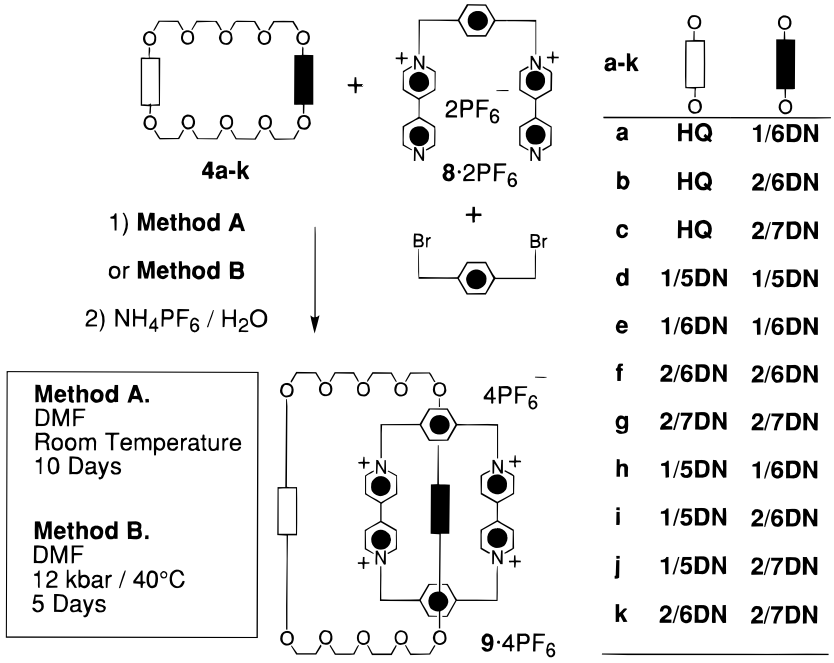

[2]catenanes **9a**−**k**·4PF_6 in yields ranging from 16 to 89%.

X-ray Crystal Structures. The X-ray crystallographic analyses of **9a**·4PF_6, **9b**·4PF_6, **9e**·4PF_6, **9h**·4PF_6, and **9j**·4PF_6 reveal, with the exception of **9e**·4PF_6, [2]catenane structures (Figures 1−5) wherein the hydroquinone or 1,5-dioxynaphthalene units are positioned inside the cavity of the tetracationic cyclophane. These geometries are consistent (*vide infra*) with those observed in solution. In all these structures, the inside OC_6H_4O or $OC_{10}H_6O$ vectors are inclined steeply with respect to the mean plane of the tetracationic cyclophane defined by the four corner methylene carbon atoms. The equivalent $OC_{10}H_6O$ vectors of the naphthalene units located alongside, however, lie close to this plane. In **9e**·4PF_6, where both naphthalene units are the same but have an asymmetric 1,6-substitution pattern, the tilt of each $OC_{10}H_6O$ vector with respect to the plane of the tetracationic cyclophane is essentially the same. The symmetric arrangement of both the inside and outside 1,6-dioxynaphthalene units in **9e**·4PF_6 may be a consequence of the inclusion of a water molecule that is hydrogen bonded within the [2]catenane and may, thus, have a perturbing effect on the conformation of the polyether linkages. Although, in all structures, the inside dioxynaphthalene ring is positioned approximately symmetrically with respect to the sandwiching pairs of bipyridinium units, there is, in most instances (the exception being **9b**·4PF_6, which has crystallographic C_2 symmetry), a noticeable offset of the alongside dioxynaphthalene unit with respect to the inside bipyridinium component. These distortions are highlighted in Figures 1−5, which show the projections of the molecules normal to the planes of the bipyridinium units. These differences in orientations of the alongside dioxynaphthalene may be

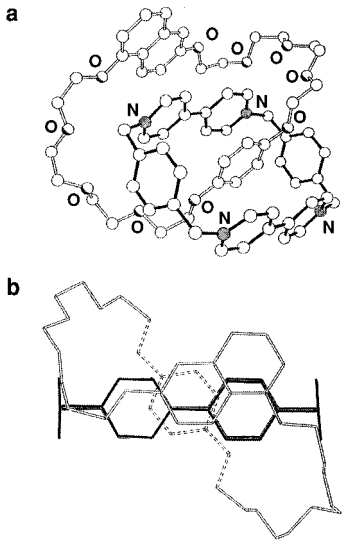

Figure 1. (a) Structure of the [2]catenane **9a**$^{4+}$ in the solid state. (b) Relative orientation of the alongside 1,6-dioxynaphthalene unit with respect to the inside bipyridinium unit within the [2]catenane **9a**$^{4+}$ in the solid state.

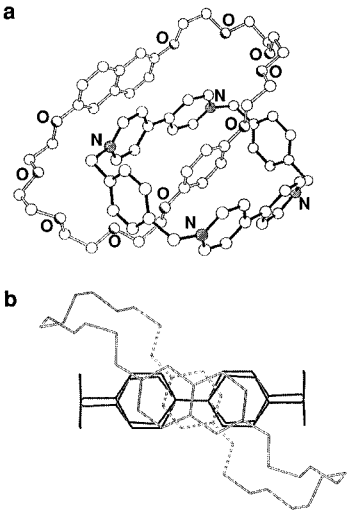

Figure 2. (a) Structure of the [2]catenane **9b**$^{4+}$ in the solid state. (b) Relative orientation of the alongside 2,6-dioxynaphthalene unit with respect to the inside bipyridinium unit within the [2]catenane **9b**$^{4+}$ in the solid state.

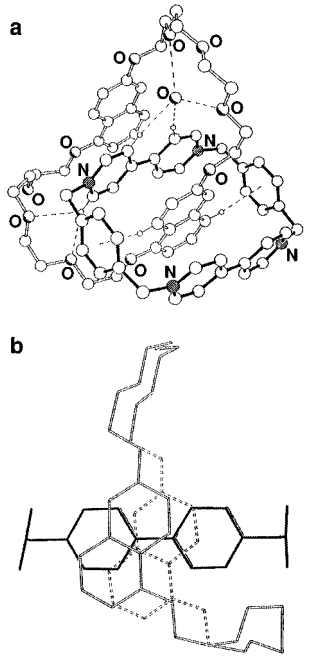

Figure 3. (a) Structure of the [2]catenane $\mathbf{9e}^{4+}$ in the solid state, showing also the [C−H···O] and [C−H···π] interactions and the positioning of the included H_2O molecule encircled by one of the polyether linkages. (b) Relative orientation of the alongside 1,6-dioxynaphthalene unit with respect to the inside bipyridinium unit within the [2]catenane $\mathbf{9e}^{4+}$ in the solid state.

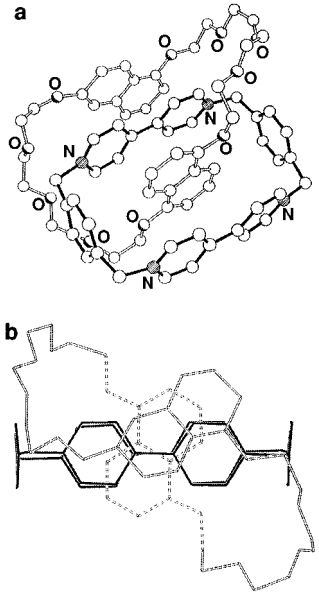

Figure 4. (a) Structure of the [2]catenane $\mathbf{9h}^{4+}$ in the solid state. (b) Relative orientation of the alongside 1,6-dioxynaphthalene unit with respect to the inside bipyridinium unit within the [2]catenane $\mathbf{9h}^{4+}$ in the solid state.

a consequence of the change of the charge distribution on the naphthalene rings as a consequence of the different substitution pattern. In all structures, the molecules pack to form polar stacks that extend along the shortest crystallographic axial direction.

Association Constants. In order to establish the ability of the tetracationic cyclophane **10**·$4PF_6$ to bind (Figure 6) regioisomeric dioxynaphthalene-based acyclic polyethers, the diols **2a**−**e** were synthesized. The association constants (K_a) (Table 1) for the corresponding

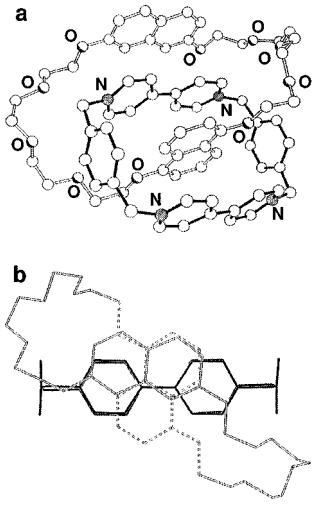

Figure 5. (a) Structure of the [2]catenane $\mathbf{9j}^{4+}$ in the solid state. (b) Relative orientation of the alongside 2,7-dioxynaphthalene unit with respect to the inside bipyridinium unit within the [2]catenane $\mathbf{9j}^{4+}$ in the solid state.

Table 1. Association Constants (K_a) and Derived Free Energies of Complexation ($-\Delta G°$) for the 1:1 Complexes [2a−e:10]·$4PF_6$ and [4a−e:PQT]·$2PF_6$ in CD_3CN at 25 °C

complex	K_a (M^{-1})	$-\Delta G°$ (kcal mol^{-1})
[**2a**:**10**]·$4PF_6$	2200[a]	4.6
[**2b**:**10**]·$4PF_6$	378[a]	3.2
[**2c**:**10**]·$4PF_6$	177[a]	3.5
[**2d**:**10**]·$4PF_6$	221[a]	3.1
[**2e**:**10**]·$4PF_6$	>5000[b]	>5
[**4a**:**PQT**]·$2PF_6$	234[c]	3.2
[**4b**:**PQT**]·$2PF_6$	469[c]	3.6
[**4c**:**PQT**]·$2PF_6$	414[c]	3.6
[**4d**:**PQT**]·$2PF_6$	1190[c]	4.2
[**4e**:**PQT**]·$2PF_6$	472[c]	3.6
[**4g**:**PQT**]·$2PF_6$	970[c]	4.1
[**4h**:**PQT**]·$2PF_6$	447[c]	3.6
[**4i**:**PQT**]·$2PF_6$	881[c]	4.0
[**4j**:**PQT**]·$2PF_6$	852[c]	4.0
[**4k**:**PQT**]·$2PF_6$	833[c]	4.0

[a] The association constants (percentage error ≤11%) were determined by ^1H NMR spectroscopy by employing the continuous variation methodology (Connors, K.A. *Binding Constants*; Wiley: New York, 1987). [b] Literature value (Asakawa, M.; Dehaen, W.; L'abbe, G.; Menzer, S.; Nouwen, J.; Raymo, F. M.; Stoddart, J. F.; Williams, D. J. *J. Org. Chem.* **1996**, *61*, 9591). [c] The association constants (percentage error ≤7%) were determined by UV−vis spectroscopy by employing the titration methodology (Connors, K. A. *Binding Constants*; Wiley: New York, 1987). In the case of [**4f**:**PQT**]·$2PF_6$, K_a was not determined as a result of the low solubility of the macrocyclic polyether **4f**.

1:1 complexes [**2a**−**e**:**10**]·$4PF_6$ were determined by ^1H NMR spectroscopy by employing the continuous variation methodology.[9] Large differences in the K_a values were observed, suggesting that the substitution pattern on the dioxynaphthalene unit has a dramatic effect upon the molecular recognition event. The differences in K_a values are directly reflected in (i) the yields of the [2]catenanes **9e**−**g**·$4PF_6$ and **9k**·$4PF_6$, which incorporate two weakly bound dioxynaphthalene units within their macrocyclic polyether component, and (ii) the translational isomerism associated with the asymmetric [2]catenanes **9a**−**c**·$4PF_6$ and **9h**−**k**·$4PF_6$ in solution and in the solid state.

In order to assess the ability of the macrocyclic polyethers **4a**−**k** to bind (Figure 7) the bipyridinium-based salt [**PQT**]·$2PF_6$, the association constants (Table 1) of

(9) Connors, K. A. *Binding Constants*; Wiley: New York, 1987.

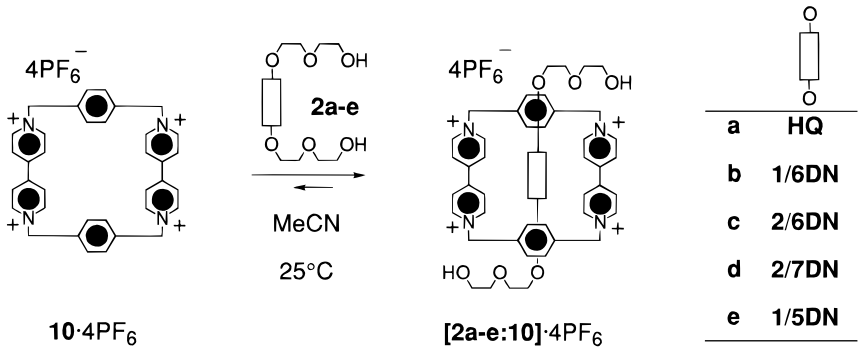

Figure 6. Complexation of the π-electron-rich acyclic polyethers **2a**−**e** by the tetracationic cyclophane **10**·4PF_6.

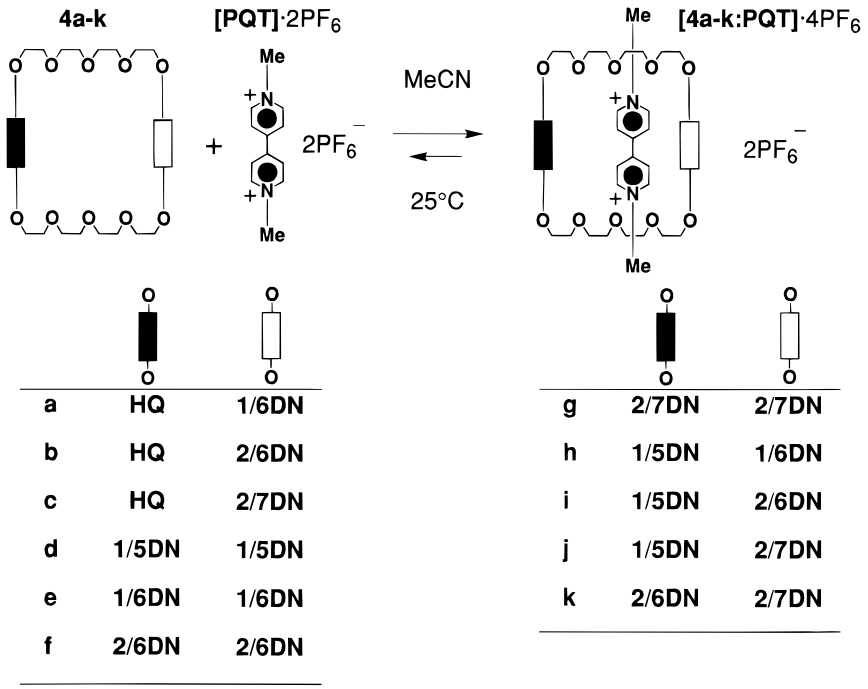

Figure 7. Complexation of [**PQT**]·2PF_6 by the π-electron-rich macrocyclic polyethers **4a**−**k**.

the corresponding 1:1 complexes were determined by UV−visible spectroscopy by employing the titration methodology[9] and following the charge-transfer band arising from the interaction between the complementary aromatic units. Again, large differences in the values of K_a, which are directly reflected in the yields of the corresponding [2]catenanes, were observed.

^{1}H NMR Spectroscopy. The ^{1}H NMR spectra of the [2]catenanes **9a**−**k**·4PF_6 display temperature dependence between 190 and 373 K in various solvents, as a result of the four dynamic processes shown in Figures 8 and 9. Process I involves the circumrotation of the macrocyclic polyether through the cavity of the tetracationic cyclophane. Similarly, process II involves the circumrotation of the tetracationic cyclophane through the cavity of the macrocyclic polyether. Exchange between the two different proton environments H_α and $H_{\alpha'}$ as well as H_β and $H_{\beta'}$ resulting from the asymmetry of the dioxynaphthalene units can occur *via* processes IIIa and IIIb. In addition, process IV is observed in [2]catenanes incorporating hydroquinone units. The free energy barriers $\Delta G_c^\ddagger$ associated with processes I−IV were derived[10] (Table 2) by variable-temperature ^{1}H NMR spectroscopic investigation. These values were determined at the coalescence temperatures T_c of the probe protons. Since the T_c values vary from one catenane to the other, direct comparisons of $\Delta G_c^\ddagger$ values should be made exercising some caution.

The [2]catenanes **9a**−**c**·4PF_6 incorporate one hydroquinone and one 1,6-, 2,6-, or 2,7-dioxynaphthalene unit within their macrocyclic polyether components, respectively. The association constant (Table 1) for the complexation of the hydroquinone-based acyclic polyether **2a** by the tetracationic cyclophane **10**·4PF_6 is approximately 1 order of magnitude higher than any of the K_a values measured for the guests **2b**−**d**—*i.e.*, the hydroquinone-based guest is bound considerably better than any of the 1,6-, 2,6-, or 2,7-dioxynaphthalene-based guests. In addition, single-crystal X-ray crystallographic analyses of the [2]catenanes **9a,b**·4PF_6 reveals (Figures 1 and 2, respectively) that only the translational isomers bearing the hydroquinone unit inside the cavity of the tetracationic cyclophane are present in the solid state. Consistently, the ^{1}H NMR spectra of the [2]catenanes **9a**−**c**·4PF_6 recorded in a range of solvents (CD_3COCD_3, CD_3CN, and CD_3SOCD_3) and temperatures (193−373 K) show resonances centered between δ 3.2 and 3.9 for the hydroquinone protons. These chemical shift values—

(10) (a) Sutherland, I. O. *Ann. Rep. NMR Spectrosc.* **1971**, *4*, 71−235. (b) Sandström, J. *Dynamic NMR Spectroscopy*; Academic Press: London, 1982.

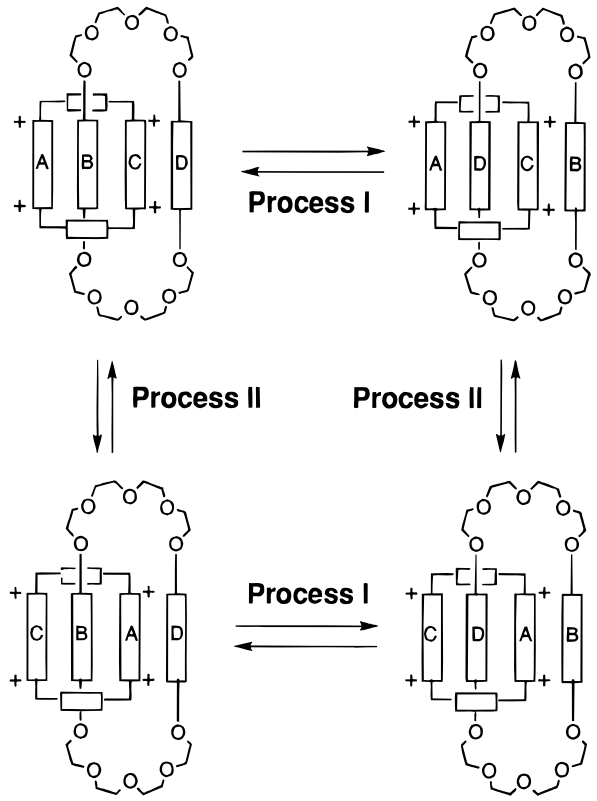

Figure 8. Dynamic processes I and II associated with the [2]-catenanes **9a**−**k**·4PF_6 in solution.

unusual for aromatic protons—demonstrate that (i) the hydroquinone unit is located exclusively inside the cavity of the tetracationic cyclophane, thus suffering significant shielding effects as a result of the sandwiching bipyridinium units, and (ii) process I cannot be observed on the ^{1}H NMR time scale. On the contrary, the free energy barriers at the coalescence temperatures associated with process II in **9a**−**c**·4PF_6 and process IV in **9a**·4PF_6 and **9c**·4PF_6 were determined (Table 2), employing the protons H_α and the hydroquinone protons as probes, respectively.

The [2]catenanes **9d**−**g**·4PF_6 incorporate two identical π-electron-rich aromatic units within their macrocyclic polyether components. The free energy barriers associated with processes I−III were determined (Table 2) for **9d**·4PF_6 and **9f,g**·4PF_6, while in the case of **9e**·4PF_6 only the $\Delta G_c^{\ddagger}$ values associated with processes I and II could be determined.

The [2]catenanes **9h**−**j**·4PF_6 incorporate one 1,5-dioxynaphthalene and one 1,6-, 2,6-, or 2,7-dioxynaphthalene unit within their macrocyclic polyether components, respectively. The association constant (Table 1) for the complexation of the 1,5-dioxynaphthalene-based acyclic polyether **2e** by the tetracationic cyclophane **10**·4PF_6 is at least 1 order of magnitude higher than any of the K_a values measured for the guests **2b**−**d**—*i.e.*, the 1,5-dioxynaphthalene-based guest is bound much better than any of the 1,6-, 2,6-, or 2,7-dioxynaphthalene-based guests. In addition, single-crystal X-ray crystallographic analyses of the [2]catenanes **9h**·4PF_6 and **9j**·4PF_6 reveals (Figures 4 and 5, respectively) that only the translational isomers bearing the 1,5-dioxynaphthalene unit inside the cavity of the tetracationic cyclophane are present in the solid state. Consistently, the ^{1}H NMR spectra of the [2]catenanes **9h**−**j**·4PF_6 recorded in a range of solvents (CD_3COCD_3 and CD_3CN) and temperatures (213−373 K) show resonances centered between δ 2.1 and 2.6 for the protons attached to the 4- and 8-positions of the 1,5-dioxynaphthalene unit. The shielding effect suffered by these protons is a result of the exclusive location of the 1,5-dioxynaphthalene unit inside the cavity of the tetracationic cyclophane. The free energy barriers associated with process II were determined (Table 2) for **9h**−**j**·4PF_6, employing the protons H_α as the probes. On the contrary, processes I and III cannot be distingushed in the case of these [2]catenanes. The $\Delta G_c^{\ddagger}$ values listed in Table 2 for these processes can only be equated with free energy barriers that result in the exchange by some mechanism or other involving process I and/or III of the probe protons.

The [2]catenane **9k**·4PF_6 incorporates one 2,6-dioxynaphthalene and one 2,7-dioxynaphthalene unit within its macrocyclic polyether component. The association constants for the binding of the 2,6-dioxynaphthalene- and 2,7-dioxynaphthalene-based acyclic polyethers **2c** and **d** by the tetracationic cyclophane **10**·4PF_6 are very similar (177 ± 18 and 221 ± 24 M^{-1}, respectively, Table 1). However, the ^{1}H NMR spectra of **9k**·4PF_6 recorded in CD_3COCD_3 and in a range of temperatures (223−273 K) reveal resonances between δ 3.2 and 3.4 for the protons attached to the 1- and 5-positions of the 2,6-dioxynaphthalene unit. These observations suggest that the 2,6-dioxynaphthalene unit is located exclusively

Table 2. Kinetic and Thermodynamic Parameters for the Dynamic Processes Associated with the [2]Catenanes 9a−k·4PF_6 in Solution

[2]catenane	protons	$\Delta\nu^a$ (Hz)	k_c^b (s^{-1})	T_c^c (K)	$\Delta G_c^{\ddagger\,d}$ (kcal mol^{-1})	process[e]
9a·4PF_6	α-CH	117	260	239[h]	11.2	II
	OC_6H_4O	1373	3047	203[h]	8.5	IV
9b·4PF_6	α-CH	142	315	243[h]	11.4	II
9c·4PF_6	α-CH	135	299	254[h]	11.9	II
	OC_6H_4O	1368	3038	245[h]	10.6	IV
9d·4PF_6	H-2/6	108	240	361[i]	17.2	I
	α-CH	24[f]	75	257[i]	12.7	II
	β-CH	63	140	327[i]	15.8	III
9e·4PF_6	H-2	66	147	278[i]	13.5	I
	α-CH	94, 82, 85, 30[g]	201	208[i]	9.8	II
9f·4PF_6	H-3/7	149	331	305[i]	14.4	I
	α-CH	22	49	226[i]	11.4	II
	α-CH	19	42	252[i]	12.8	III
9g·4PF_6	H-3/6	267	593	302[h]	13.9	I
	CH_2-N^+	40	89	182[h]	8.9	II
	α-CH	42	93	241[h]	11.8	III
9h·4PF_6	C_6H_4	47	104	311[i]	15.4	I/III
	α-CH	47	104	227[h]	11.1	II
9i·4PF_6	α-CH	110	245	349[i]	16.7	I/III
	α-CH	67	149	242[h]	11.7	II
9j·4PF_6	α-CH	158	349	354[i]	16.7	I/III
	α-CH	158	351	245[h]	11.5	II
9k·4PF_6	β-CH	95	211	277[h]	13.2	I/III
	β-CH	158	351	237[h]	11.0	II

[a] Limiting frequency separation. [b] Rate constant at coalescence. [c] Temperature of coalescence. [d] Free energy of activation at the coalescence temperature. [e] The dynamic processes associated with the [2]catenanes **9a**−**k**·4PF_6 are schematically illustrated in Figures 8 and 9. [f] The line width methodology was employed to determine the kinetic and thermodynamic parameters (Sandström, J. *Dynamic NMR Spectroscopy*; Academic Press: London, 1981). [g] Differences between the frequencies of the resonances associated with the exchanging pairs of α- and β-protons on the bipyridinium units. These signals were assigned by a saturation transfer experiment performed at 198 K. Line-shape analysis was employed to determine the kinetic and thermodynamic parameters (Sandström, J. *Dynamic NMR Spectroscopy*; Academic Press: London, 1981). [h] In CD_3COCD_3. [i] In CD_3CN. [j] In CD_3COCD_3/CD_3CN (7:3).

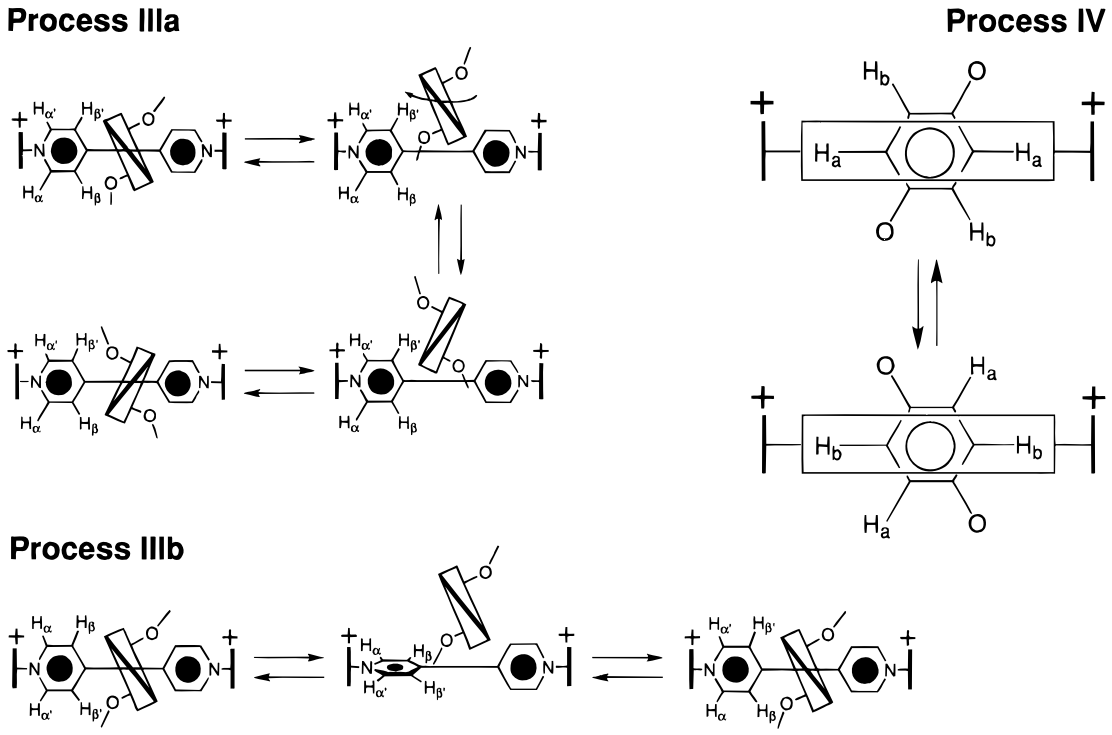

Figure 9. Dynamic processes IIIa, IIIb, and IV associated with the [2]catenanes **9a**−**k**·4PF_6 in solution.

Table 3. Electrochemical Data Associated with the [2]Catenanes 9a−k·4PF_6 and the Tetracaionic Cyclophane 10·4PF_6

compd	E_1[a] (mV)	E'_1[a] (mV)	E_2[a] (mV)	half width[b] (mV)	$\Delta E_{1/2}$[c] (mV)	K_c[d]
9a·4PF_6	−296	−412	−853	124	98.9	47.0
9b·4PF_6	−302	−408	−865	110	86.5	29.0
9c·4PF_6	−302	−410	−849	116	91.8	35.6
9d·4PF_6[e]	−354	−572	−861	250	210	3548.9
9e·4PF_6	−274	−378	−848	122	97.1	−43.8
9g·4PF_6	−274	−378	−841	102	79.4	22.0
9h·4PF_6	−317	−436	−857	125	99.8	48.6
9i·4PF_6	−330	−433	−875	107	83.9	26.2
9j·4PF_6	−320	−429	−840	109	85.6	28.0
9k·4PF_6	−270	−364	−854	−104	81.2	23.6
10·4PF_6[e]	−283		−708	59.7	40.2	0.21

[a] Reduction potentials. [b] The half-width ($E_p - E_{p/2}$) values were measured on the first reduction peak of the voltammogram (Richardson, D. E.; Taube, H. *Inorg. Chem.* **1981**, *20*, 1278−1285). [c] Difference between the two [bipyridinium]$^{2+}$/[[bipyridinium]$^{+}$ half-wave potentials. [d] Equilibrium conproportionation constant for the process $X^{2+} + X^{4+} = 2X^{3+}$, where X may be any of the bipyridinium-based compounds, calculated from the expression $K_c = \exp[(\Delta E_{1/2})F/RT]$. [e] Literature values (Ashton, P. R.; Brown, C. L.; Chrystal, E. J. T.; Goodnow, T. T.; Kaifer, A. E.; Parry, K. P.; Philp, D.; Slawin, A. M. Z.; Spencer, N.; Stoddart, J. F.; Williams, D. J. *J. Chem. Soc., Chem. Commun.* **1991**, 634−639).

inside the cavity of the tetracationic cyclophane. As in the case of the [2]catenanes **9h**−**j**·4PF_6, the free energy barriers for process II and a $\Delta G_c^{\ddagger}$ value associated with the combination of processes I and III were determined (Table 2) for **9k**·4PF_6.

Electrochemistry. Cyclic voltammetry of the tetracationic cylcophane **10**·4PF_6 shows[7a,11] (Table 3) two reversible reduction processes with half-wave potentials of −283 and −708 mV corresponding to two-electron reductions of the couples [bipyridinium]$^{2+}$/[bipyridinium]$^{+}$ and [bipyridinium]$^{+}$/[bipyridinium], respectively. These observations suggest that the two bipyridinium units of the tetracationic cyclophane **10**·4PF_6 are reduced simultaneously as a result of two consecutive additions of two electrons. On the contrary, when the tetracationic cyclophane is mechanically-interlocked within the [2]catenanes **9**·4PF_6, the two bipyridinium units are no longer equivalent. The bipyridinium unit located inside the cavity of the π-electron-rich macrocyclic polyether is reduced at more negative potentials as a result of the stabilizing $\pi-\pi$ stacking interactions with the two π-electron-rich aromatic units incorporated within the macrocyclic polyether. Thus, cyclic voltammetry of the [2]catenanes **9**·4PF_6 shows three reversible reduction processes. The first two processes are monoelectronic reductions of the alongside and inside bipyridinium units, respectively, while the third process is a two-electron addition corresponding to the almost simultaneous reduction of the two bipyridinium radical cations. Presumably, once both bipyridinium units are monoelectronically reduced their acceptor character is diminished and alongside and inside units are no longer distinguishable and so are reduced almost simultaneously with the second electrons. Interestingly, the difference between the reduction potentials of the alongside (E_1) and inside (E'_1) bipyridinium units is significantly larger (218 mV) in the case of the [2]catenane **9d**·4PF_6[11] incorporating two 1,5-dioxynaphthalene units within its macrocyclic polyether component. This result suggests that the strongest donor−acceptor interactions are achieved when the 1,5-dioxynaphthalene unit is employed, consistent with the association constants (Table 1) measured in solution for the pseudorotaxanes [**2a**−**e**:**10**]·4PF_6 and with the selectivity associated with the translational isomersim that characterizes the asymmetric [2]catenanes **9h**−**j**·4PF_6.

Conclusions

A series of novel π-electron-rich symmetric and asymmetric macrocyclic polyethers incorporating hydroqui-

(11) Ashton, P. R.; Brown, C. L.; Chrystal, E. J. T.; Goodnow, T. T.; Kaifer, A. E.; Parry, K. P.; Philp, D.; Slawin, A. M. Z.; Spencer, N.; Stoddart, J. F.; Williams, D. J. *J. Chem. Soc., Chem. Commun.* **1991**, 634−639

none and/or dioxynaphthalene units have been prepared efficiently *via* two-step synthetic procedures. These macrocycles bind the bipyridinium-based bis(hexafluorophosphate) salt, paraquat, as a result of $\pi-\pi$ stacking interactions between the complementary aromatic units as well as of hydrogen bonding interactions between the polyether oxygen atoms and the acidic hydrogen atoms on the bipyridinium units. Similarly, the complexation of hydroquinone- and dioxynaphthalene-based acyclic polyethers—the acyclic counterparts of the macrocyclic polyethers—by the bipyridinium-based cyclophane cyclobis(paraquat-*p*-phenylene) occurs in solution. However, significant differences in the values of the association constants were observed on varying the nature and the substitution pattern of the aromatic unit, incorporated within the π-electron-rich polyethers. The dramatic differences in the association constants are directly reflected in (i) the yields of the self-assembling processes leading to [2]catenanes incorporating the macrocyclic polyethers and cyclobis(paraquat-*p*-phenylene) and (ii) the translational isomerism associated with these [2]-catenanes. In a number of cases, only one of the two possible translational isomers expected for those [2]-catenanes incorporating asymmetric macrocyclic polyethers is observed both in solution and in the solid state, as demonstrated by variable-temperature ^{1}H NMR spectroscopic investgation and single-crystal X-ray crystallographic analyses, respectively. The X-ray crystallographic analyses also revealed that, upon varying the substitution pattern (1,5-, 2,6-, and 2,7-) on the dioxynaphthalene units, dramatic changes in the relative orientation of these units with respect to the bipyridinium units is observed within the [2]catenanes. These changes are undoubtedly a result of the difference in the stereoelectronic features possessed by each regioisomeric dioxynaphthalene unit that govern the geometry of the $\pi-\pi$ stacking interactions. We believe that this investigation demonstrates how subtle changes in the stereoelectronic information imprinted within simple molecular components can dramatically affect their molecular recognition, both in solution and in the solid state, as well as the efficiencies of self-assembly processes leading to them in the first place.

Experimental Section

General Methods. The starting materials were purchased from commercial sources and used without further purification, unless otherwise mentioned. Dimethylformamide (DMF) and acetonitrile (MeCN) were distilled from calcium hydride prior to use. Tetraethylene glycol dichloride,[12] tetraethylene glycol bistosylate,[7a] diethylene glycol monotosylate,[13] the diols **2a**[7a] and **2e**,[14] 1,5-dinaphtho-38-crown-10 **4d**,[15] the bis(hexafluorophosphate) salt **8**·2PF$_6$,[7a] and the teracationic cyclophane **10**·4PF$_6$[7a] were prepared according to literature procedures. Thin-layer chromatography (TLC) was carried out on aluminum plates, coated either with silica gel or with neutral alumina. Compounds were detected by UV light or by development with either of the following: (a) solution containing 25 g of phosphomolybdic acid, 10 g of cerium(IV) sulfate·4H$_2$O, 60 mL of concd H$_2$SO$_4$ and 940 mL of H$_2$O, or (b) I$_2$/I$^-$ in EtOH/H$_2$O. Flash column chromatography[16] (FCC) was performed either on silica gel or on basic alumina using a pressure of 0.2−0.5 bar with the solvents specified. Melting points are uncorrected. Reactions requiring ultrahigh pressures were carried out in Teflon vessels using a custom-built ultrahigh-pressure press. Electron impact (EI) mass spectra were performed at 70 eV, and chemical ionization (CI) mass spectra were obtained employing NH$_3$. Low-resolution liquid secondary ion mass spectrometry (LSIMS) spectra were obtained utilizing a *m*-nitrobenzyl alcohol (NOBA) matrix and magnet scanning at 5 s per decade. High-resolution accurate mass measurements using LSIMS were obtained operating at a resolution of 6000 and employing narrow range voltage scanning and a reference of cesium and rubidium iodides mixed in equimolar proportions. ^{1}H nuclear magnetic resonance (NMR) spectra were recorded at either 300 or 400 MHz. ^{13}C NMR spectra were recordrd at either 75 or 100 MHz using the JMOD pulse sequence. UV−vis spectra were measured at 25 °C in Me$_2$CO.

General Procedure for the Synthesis of Naphthalene-Based Diols 2b−d. A solution of **1b−d** (0.02 mol) in dry DMF (20 mL) was added to a stirred suspension of K$_2$CO$_3$ (8.3g, 0.06 mol) in dry DMF (50 mL) under nitrogen. The reaction mixture was heated to 60 °C with vigorous stirring for 1 h. Diethylene glycol monotosylate (13.5 g, 0.052 mol) in dry DMF (30 mL) was added over 20 min, and the temperature was raised to 80 °C. After 6 days, the reaction mixture was cooled to room temperature and filtered, and the solid was washed with CH$_2$Cl$_2$. The combined filtrate was evaporated *in vacuo* and the residue partitioned between CH$_2$Cl$_2$ and 5% aqueous HCl. The organic layer was separated, washed with H$_2$O and brine, and dried (MgSO$_4$). Filtration and evaporation gave the crude product, which was subjected to FCC on alumina using the solvents specified.

1,6-Bis[2-(hydroxyethoxy)ethoxy]naphthalene (2b): eluent CH$_2$Cl$_2$/MeOH/NH$_4$OH 100/5/1; yield 71%; viscous oil; ^{1}H NMR (300 MHz, CD$_3$CN) δ 2.97 (m, 2H), 3.54−3.67 (m, 8H), 3.80 (m, 2H), 3.87 (m, 2H), 4.17 (t, 2H, J = 5 Hz), 4.21 (t, 2H, J = 5 Hz), 6.73 (t, 1H, J = 5 Hz), 7.12 (dd, 1H, J = 9, 2.5 Hz,), 7.19 (d, 1H, J = 2.5 Hz), 7.33 (d, 2H, J = 5 Hz), 8.14 (d, 1H, J = 9 Hz); ^{13}C NMR (75 MHz, CD$_3$CN) δ 62.1, 62.1, 68.5, 68.9, 70.3, 70.4, 73.6, 73.7, 104.5, 107.8, 118.6, 120.4, 121.7, 124.6, 128.0, 137.1, 155.7, 158.3; EIMS *m*/*z* (rel intens) 336 (34) [M]$^+$, 248 (11), 160 (63), 131 (16), 89 (14), 45 (100). Anal. Calcd for C$_{18}$H$_{24}$O$_6$: C, 64.27; H, 7.19; Found: C, 64.30; H, 7.21.

2,6-Bis[2-(2-hydroxyethoxy)ethoxy]naphthalene (2c): eluent CH$_2$Cl$_2$/MeOH/NH$_4$OH 100/2.5/0.5; yield 62%; mp 126−127 °C (EtOAc−light petroleum); ^{1}H NMR (300 MHz, CD$_3$CN) δ 2.74 (t, 2H, J = 5.5 Hz), 3.55−3.64 (m, 8H), 3.84 (m, 4H), 4.20 (m, 4H), 7.13 (dd, 2H, J = 9, 2.5 Hz), 7.23 (d, 2H, J = 2.5 Hz), 7.69 (d, 2H, J = 9 Hz); ^{13}C NMR (75 MHz, CD$_3$CN, 338 K) δ 62.4, 69.0, 70.6, 73.8, 108.8, 108.9, 120.2, 120.3, 129.4, 129.4, 131.2, 156.7; EIMS *m*/*z* (rel intens) 336 (23) [M]$^+$, 248 (5), 160 (41), 131 (7), 89 (6), 45 (100). Anal. Calcd for C$_{18}$H$_{24}$O$_6$: C, 64.27; H, 7.19. Found: C, 64.27; H, 7.22.

2,7-Bis[2-(2-hydroxyethoxy)ethoxy]napthalene (2d): eluent CH$_2$Cl$_2$/MeOH/NH$_4$OH 100/5/1; yield 82%; mp 70−71 °C (EtOAc−light petroleum); ^{1}H NMR (300 MHz, CDCl$_3$) δ 2.88 (s, 2H), 3.66 (t, 4H, J = 5 Hz), 3.76 (t, 4H, J = 5 Hz), 3.86 (t, 4H, J = 5 Hz), 4.17 (t, 4H, J = 5 Hz), 6.99−7.04 (m, 4H), 7.62 (d, 2H, J = 10 Hz); ^{13}C NMR (75 MHz, CDCl$_3$) δ 61.7, 67.4, 69.6, 72.7, 106.4, 116.4, 129.2, 124.6, 135.8, 157.3; CIMS (NH$_3$) *m*/*z* (rel intens) 354 (13) [M + NH$_4$]$^+$, 337 (100) [M + H]$^+$, 293 (57), 275 (20), 249 (85), 233 (34), 205 (48),187 (32),160 (81), 144 (38), 89 (72). Anal. Calcd for C$_{18}$H$_{24}$O$_6$: C, 64.27; H, 7.19. Found: C, 63.98; H, 6.90. A second fraction gave **2-hydroxy-7-[2-(2-hydoxyethoxy)ethoxy]napthalene** (8%): mp 131−132 °C; ^{1}H NMR (300 MHz, CD$_3$SOCD$_3$) δ 3.52 (m, 4H), 3.78 (t, 2H, J = 5 Hz), 4.16 (t, 2H), 4.69 (t, 1H, J = 5 Hz), 6.90 (dt, 2H, J = 9 Hz, J = 2 Hz), 7.03 and 7.10 (each d, 1H, J = 2 Hz), 7.65 (dd, 2H, J = 9, 2 Hz), 9.67 (s, 1H); ^{13}C NMR (75 MHz, CD$_3$COCD$_3$) δ 60.4, 67.2, 69.0, 72.6, 105.4, 108.2, 115.3, 116.0, 129.1, 129.1, 123.2, 136.1, 155.9, 156.8; CIMS (NH$_3$) *m*/*z* (rel

(12) Pedersen, C. J. *J. Am. Chem. Soc.* **1967**, *89*, 7017−7035.
(13) Börjesson, L.; Welch, C. J. *Acta Chem. Scand.* **1991**, *45*, 621−626.
(14) Ashton, P. R.; Blower, M.; Philp, D.; Spencer, N.; Stoddart, J. F.; Tolley, M. S.; Ballardini, R.; Ciano, M.; Balzani, V.; Gandofi, M. T.; Prodi, L. *New. J. Chem.* **1993**, *17*, 689−695.
(15) Ashton, P. R.; Chrystal, E. J. T.; Mathias, J. P.; Parry, K. P.; Slawin, A. M. Z.; Spencer, N.; Stoddart, J. F.; Williams, D. J. *Tetrahedron Lett.* **1987**, *28*, 6367−6370.
(16) Still, W. C.; Kahn, M.; Mitra, A. *J. Org. Chem.* **1978**, *43*, 2923−2925.

intens) 266 (44) $[M + NH_4]^+$, 249 (100) $[M + H]^+$, 205 (30), 187 (22), 176 (46), 160 (76), 144 (46), 131 (53), 115 (32). Anal. Calcd for $C_{14}H_{16}O_4$: C, 67.72; H, 6.50. Found: C, 67.75; H, 6.50.

General Procedure for the Synthesis of Dichlorides 3a−d. A mixture of the corresponding arenediol **1a−d** (0.05 mol), tetraethylene glycol dichloride (230 g, 1.0 mol), and K_2CO_3 (16.5 g, 0.12 mol) in 200 mL of dry MeCN was refluxed for 48 h. The mixture was cooled to room temperature, and the salts were filtered off and washed with CH_2Cl_2. The combined filtrate was concentrated on a rotory evaporator (to remove volatile solvents), and then the excess of dichloride was distilled off at reduced pressure (about 204 g, 98 °C/0.05 Torr). The oily residue was purified by FCC on silica gel or crystallized to give the pure dichlorides **3a−d**.

1,4-Bis[2-[2-[2-(2-chloroethoxy)ethoxy]ethoxy]ethoxy]-benzene (3a): eluent CH_2Cl_2/MeOH 100/3; yield 88%; a viscous oil; ^{1}H NMR (300 MHz, $CDCl_3$) δ 3.59−3.64 (m, 4H), 3.66−3.77 (m, 20H), 3.80−3.85 (m, 4H), 4.07 (t, 4H, J = 5 Hz), 6.83 (s, 4H); ^{13}C NMR(75 MHz, $CDCl_3$) δ 42.7, 68.1. 69.9, 70.6, 70.7, 70.7, 70.8, 71.4, 115.6, 153.1; LSIMS m/z 498 $[M]^+$. Anal. Calcd for $C_{22}H_{36}O_8Cl_2$: C, 52.91; H, 7.27. Found: C, 53.10; H, 7.27.

1,6-Bis[2-[2-[2-(chloroethoxy)ethoxy]ethoxy]ethoxy]-naphthalene (3b): eluent CH_2Cl_2/MeOH 100/2; yield 81%; a viscous oil; ^{1}H NMR (300 MHz, $CDCl_3$) δ 3.61 (m, 4H), 3.65−3.81 (m, 20 H), 3.91 (t, 2H, J = 5 Hz), 3.98 (t, 2H, J = 5 Hz), 4.24 (t, 2H, J = 5 Hz), 4.28 (t, 2H, J = 5 Hz), 6.67 (dd, 1H, J = 6 Hz), 7.09 (d, 1H, J = 2.5 Hz), 7.14 (dd, 1H, J = 9, 2.5 Hz), 7.27−7.35 (m, 2H), 8.18 (d, 1H, J = 9 Hz); ^{13}C NMR (75 MHz, $CDCl_3$) δ 42.7, 67.4, 67.8, 69.7, 69.8, 70.6, 70.7, 70.7, 70.8, 71.0, 71.3, 103.2, 106.7, 117.8, 119.4, 123.8, 126.6, 121.0, 135.9, 154.7, 157.3; LSIMS m/z 548 $[M]^+$. Anal. Calcd for $C_{26}H_{38}O_8Cl_2$: C, 56.83; H, 6.97. Found: C, 56.76; H, 7.00.

2,6-Bis[2-[2-[2-(chloroethoxy)ethoxy]ethoxy]ethoxy]-naphthalene (3c): eluent CH_2Cl_2/MeOH 100/3; yield 89%; mp 76−77 °C; ^{1}H NMR (300 MHz, $CDCl_3$) δ 3.60 (m, 4H), 3.64−3.77 (m, 20H), 3.90 (t, 4H, J = 5 Hz), 4.21 (t, 4H, J = 5 Hz), 7.09 (d, 2H, J = 2.5 Hz), 7.15 (dd, 2H, J = 9, 2.5 Hz), 7.61 (d, 2H, J = 9 Hz); ^{13}C NMR (75 MHz, $CDCl_3$) δ 42.7, 67.5, 69.8, 70.6, 70.7, 70.8, 71.3, 107.2, 119.2, 128.1, 129.8, 155.3; LSIMS m/z 548 $[M]^+$. Anal. Calcd for $C_{26}H_{38}O_8Cl_2$: C, 56.83; H, 6.97. Found: C, 56.73; H, 6.99.

2,7-Bis[2-[2-[2-(chloroethoxy)ethoxy]ethoxy]ethoxy]-naphthalene (3d): eluent CH_2Cl_2/MeOH 100/3; R_f = 0.48; yield 87%; a viscous oil; ^{1}H NMR (300 MHz, $CDCl_3$) δ 3.59 (m, 4H), 2.63−3.75 (m, 20H), 3.89 (t, 4H, J = 5 Hz), 4.21 (t, 4H, J = 5 Hz), 6.97−7.05 (m, 4H), 7.62 (d, 2H, J = 9 Hz); ^{13}C NMR (75 MHz, $CDCl_3$) δ 42.8, 67.4, 69.7, 70.6, 70.7, 70.9, 71.3, 106.3, 116.4, 129.1, 124.5, 135.8, 157.4; LSIMS m/z 548 $[M]^+$. Anal. Calcd for $C_{26}H_{38}O_8Cl_2$: C, 56.83; H, 6.97. Found: C, 57.19; H, 6.89. A second fraction (R_f = 0.35) gave **1,11-bis-[2-naphthoxy-7-[2-[2-[2-(2-chloroethoxy)ethoxy]ethoxy]-ethoxy]-3,6,9-trioxaundecane**: yield 3%; viscous oil; ^{1}H NMR (300 MHz, $CDCl_3$) δ 3.57−3.63 (m, 4H), 3.63−3.77 (m, 28H), 3.90 (m, 8H), 4.20 (t, 8H, J = 5 Hz), 6.98−7.05 (m, 8H), 7.62 (m, 4H); ^{13}C NMR (75 MHz, $CDCl_3$) δ 42.7, 67.4, 69.7, 70.6, 70.7, 70.8, 71.3, 106.3, 116.4, 129.1, 124.4, 135.7, 157.3; LSIMS m/z 866 $[M]^+$.

General Procedure for the Synthesis of Crown Ethers 4a−c and 4f−k. A solution of the corresponding dichloride **3** (0.01 mol) in dry MeCN (200 mL) and a solution of the corresponding arenediol **1** (0.01 mol) in dry MeCN (200 mL) were added simutaneously under nitrogen atmosphere over a period of 7 h to a stirred suspension of Cs_2CO_3 (16.3 g, 0.05 mol) and NaI (3.3 g, 0.022 mol) in MeCN (450 mL) heated at reflux. The reaction mixture was heated at reflux for a further 10 days. After cooling, the reaction mixture was filtered through Celite, the solid was washed with $CHCl_3$, and the combined filtrate was concentrated *in vacuo*. The residue was partitioned between H_2O and $CHCl_3$, and the organic layer was separated and dried ($MgSO_4$). After removal of the solvent, the crude products were purified by FCC on silica gel.

1,6-Naphthoparaphenylene-35-crown-10 (4a). From **3a** and **1b**: eluent hexane/Me_2CO 3/2; yield 18%; a viscous oil; ^{1}H NMR (300 MHz, $CDCl_3$) δ 3.64−3.87 (m, 22H), 3.89−4.03 (m, 6H), 4.17 (m, 2H), 4.28 (m, 2H), 6.65−6.72 (m, 1H), 6.64, 6.67, 6.70, 6.73 (AB sysytem, 4H), 6.97 (d, 1H, J = 2.5 Hz), 7.11 (dd, 1H, J = 7, 2.5 Hz), 7.27 (d, 1H, J = 7 Hz), 7.30 (d, 1H, J = 7 Hz), 8.17 (d, 1H, J = 9 Hz); ^{13}C NMR (75 MHz, $CDCl_3$) δ 67.6, 68.0, 69.7, 69.8, 70.8, 70.9, 71.2, 103.1, 106.8, 115.5, 115.6, 117.8, 119.4, 123.9, 126.6, 121.0, 135.9, 153.0, 154.8, 157.3; LSIMS m/z 586 $[M + H]^+$. Anal. Calcd for $C_{32}H_{42}O_{10}$: C, 65.51; H, 7.39. Found: C, 65.22; H, 7.10.

2,6-Naphthoparaphenylene-36-crown-10 (4b). From **3a** and **1c**: eluent hexane/Me_2CO 3/2; yield 15%; mp 130−131 °C; ^{1}H NMR (300 MHz, $CDCl_3$) δ 3.66−3.73 (m, 12H), 3.74−3.81 (m, 12H), 3.94 (m, 4H), 4.18 (m, 4H), 6.51 (s, 4H), 7.04 (d, 2H, J = 2.5 Hz), 7.14 (dd, 2H, J = 9, 2.5 Hz), 7.53 (d, 2H, J = 9 Hz); ^{13}C NMR (75 MHz, $CDCl_3$) δ 67.7, 67.9, 69.7, 69.8, 70.6, 70.8, 70.9, 107.3, 115.3, 119.3, 128.2, 129.8, 152.9, 155.4; LSIMS m/z 586 $[M + H]^+$. Anal. Calcd for $C_{32}H_{42}O_{10}$: C, 65.51; H, 7.39. Found: C, 65.17; H, 7.19.

2,7-Naphthoparaphenylene-35-crown-10 (4c). From **3a** and **1d**: eluent hexane/Me_2CO 3/2; yield 27%; mp 106−107 °C; ^{1}H NMR (300 MHz, $CDCl_3$) δ 3.67−3.72 (m, 12H), 3.75 (m, 8H), 3.87 (m, 4H), 3.92 (m, 4H), 4.16 (m, 4H), 6.64 (s, 4H), 6.97 (d, 2H, J = 2 Hz), 7.02 (dd, 2H, J = 9, 2 Hz), 7.62 (d, 2H, J = 9 Hz); ^{13}C NMR (75 MHz, $CDCl_3$) δ 67.5, 68.1, 69.7, 69.8, 70.7, 70.8, 70.9, 70.9, 106.2, 115.5, 116.5, 129.1, 124.4, 135.9, 153.0, 157.5; LSIMS m/z 586 $[M]^+$. Anal. Calcd for $C_{32}H_{42}O_{10}$: C, 65.51; H, 7.22. Found: C, 65.72; H, 7.39.

2,6-Dinaphtho-38-crown-10 (4f). From **3c** and **1c**: eluent CH_2Cl_2/MeOH 100/2; yield 18%; mp 169−171 °C; ^{1}H NMR (400 MHz, $CDCl_3$, 318 K) δ 3.72−3.75 (m, 16H), 3.72−3.75 (m, 8H), 4.05−4.08 (m, 8H), 6.87 (d, 2H, J = 2.6 Hz), 7.01 (dd, 2H, J = 9, 2.6 Hz), 7.33 (d, 2H, J = 9 Hz); ^{13}C NMR (67.5 MHz, CD_3SOCD_3, 368 K) δ 67.2, 68.6, 69.6, 69.7, 107.2, 118.3, 127.5, 129.0, 154.6; LSIMS m/z 636 $[M]^+$. Anal. Calcd for $C_{36}H_{44}O_{10}$: C, 67.91; H,6.97. Found: C, 67.82; H, 7.02.

2,7-Dinaphtho-36-crown-10 (4g). From **3d** and **1d**: eluent CH_2Cl_2/MeOH 100/2; yield 24%; mp 143−144 °C; ^{1}H NMR (300 MHz, $CDCl_3$) δ 3.72 (m, 16H), 3.86 (m, 8H), 4.08 (m, 8H), 6.86 (d, 4H, J = 2 Hz), 6.99 (dd, 4H, J = 9, 2 Hz), 7.55 (d, 4H, J = 9Hz); ^{13}C NMR (75 MHz, $CDCl_3$) δ 67.4, 69.7, 70.8, 70.9, 106.1, 116.5, 129.1, 124.4, 135.8, 157.4; LSIMS m/z 636 $[M]^+$. Anal. Calcd for $C_{36}H_{44}O_{10}$: C, 67.91; H,6.97. Found: C, 67.61; H, 6.91.

1,5-Naphtho-1/6-naphtho-37-crown-10 (4h). From **3b** and **1e**: eluent CH_2Cl_2/MeOH 100/2; yield 19%; a slightly yellow viscous oil; ^{1}H NMR (400 MHz, CD_3COCD_3, 303 K) δ 3.61−3.73 (m, 16H), 3.77 (m, 2H), 3.86 (m, 2H), 3.89−3.94 (m, 4H), 4.04−4.09 (m, 4H), 4.15 (m, 2H), 4.23 (m, 2H), 6.67 (dd, 1H, J = 9, 2.5 Hz), 6.72 (dd, 1H, J = 9, 2.5 Hz), 6.74 (t, 1H, J = 5 Hz), 6.97 (dd, 1H, J = 9, 2.5 Hz), 7.15 (d, 1H, J = 2.5 Hz), 7.26 (t, 1H, J = 9 Hz), 7.27 (t, 1H, J = 9 Hz), 7.30 (d, 2H, J = 5 Hz), 7.80 (dd, 1H, J = 9, 2 Hz), 7.81 (dd, 1H, J = 9, 2 Hz), 8.08 (d, 1H, J = 9 Hz); ^{13}C NMR (75 MHz, CD_3COCD_3) δ 68.1, 68.6, 68.8, 70.1, 70.1, 70.3, 71.3, 71.3, 71.3, 71.4, 71.4, 71.5, 103.7, 106.4, 106.4, 107.4, 115.0, 118.1, 119.9, 124.3, 125.8, 125.8, 127.4, 121.5, 127.5, 136.8, 155.0, 155.1, 155.5, 158.1; LSIMS m/z 636 $[M]^+$. Anal. Calcd for $C_{36}H_{44}O_{10}$: C, 67.91; H, 6.97. Found: C, 67.65; H, 7.01.

1,5-Naphtho-2/6-naphtho-36-crown-10 (4i). From **3c** and **1e**: eluent CH_2Cl_2/MeOH 100/2; yield 22%; mp 126−127 °C; ^{1}H NMR (300 MHz, $CDCl_3$) δ 3.64−3.70 (m, 8H), 3.88−3.95 (m, 4H), 3.99−4.10 (m, 4H), 6.46 (d, 2H, J = 7.5 Hz), 6.88 (d, 2H, J = 2.5 Hz), 7.06 (dd, 2H, J = 9, 2.5 Hz), 7.13 (t, 2H, J = 7.5 Hz), 7.40 (d, 2H, J = 9 Hz), 7.78 (d, 2H, J = 7.5 Hz); ^{13}C NMR (75 MHz, $CDCl_3$) δ 67.6, 67.8, 69.7, 69.8, 70.9, 71.0, 105.5, 107.2, 114.5, 119.2, 125.0, 128.1, 126.7, 129.7, 154.3, 155.3; LSIMS m/z 636 $[M]^+$; HRLSIMS calcd for $C_{36}H_{44}O_{10}$ $[M^+]$ m/z 636.2934, found m/z 636.2958.

1,5-Naphtho-2/7-naphtho-37-crown-10 (4j). From **3d** and **1e**: eluent CH_2Cl_2/MeOH 100/2; yield 17%; mp 95−96 °C; ^{1}H NMR (300 MHz, $CDCl_3$) δ 3.69−3.81 (m, 16H), 3.87 (m, 4H), 3.93 (m, 4H), 4.02 (m, 4H), 4.11 (m, 4H), 6.60 (d, 2H, J = 8 Hz), 6.78 (d, 2H, J = 2.5 Hz), 6.99 (dd, 2H, J = 9, 2.5 Hz), 7.25 (t, 2H, J = 8 Hz), 7.60 (d, 2H, J = 9 Hz), 7.85 (d, 2H, J = 8 Hz); ^{13}C NMR (75 MHz, $CDCl_3$) δ 67.4, 68.1, 69.7, 69.8, 70.8, 71.0, 105.6, 106.2, 114.6, 116.4, 125.1, 129.0, 124.4, 126.8,

135.8, 154.4, 157.3; LSIMS *m/z* 636 $[M]^+$. Anal. Calcd for $C_{36}H_{44}O_{10}$: C, 67.91; H, 6.97. Found: C, 67.59; H, 7.02.

2,6-Naphtho-2/7-naphtho-37-crown-10 (4k). From **3c** and **1d**: eluent CH_2Cl_2/MeOH 100/2; yield 21%; mp 115−116 °C (hexane/EtOAc); ^{1}H NMR (400 MHz, CD_3COCD_3) δ 3.66 (m, 16H), 3.85 (t, 4H, J = 5 Hz), 3.86 (t, 4H, J = 5 Hz), 4.07 (t, 4H, J = 5 Hz), 4.12 (t, 4H, J = 5 Hz), 6.96 (dd, 2H, J = 9, 2 Hz), 6.99 (d, 2H, J = 2 Hz), 7.03 (dd, 2H, J = 9, 3 Hz), 7.05 (d, 2H, J = 3 Hz), 7.47 (d, 2H, J = 9 Hz), 7.63 (d, 2H, J = 9 Hz); ^{13}C NMR (75 MHz, $CDCl_3$) δ 67.4, 67.7, 69.7, 69.7, 70.7, 70.8, 71.0, 106.1, 107.1, 116.5, 119.2, 128.1, 129.0, 124.4, 129.7, 135.8, 155.3, 157.4; LSIMS *m/z* 636 $[M]^+$. Anal. Calcd for $C_{36}H_{44}O_{10}$: C, 67.91; H, 6.97. Found: C, 67.96; H, 6.72.

Preparation of 1,6-Dinaphtho-36-crown-10 (4e). Benzyl bromide (34.5 g, 0.225 mol) was added to a slurry of **1b** (24.0 g, 0.15 mol) and anhydrous K_2CO_3 (27.0 g, 0.195 mol) in dry DMF (300 mL). The mixture was stirred for 20 h at 50 °C under nitrogen. The inorganic solids were removed by filtration, and the filtrate was concentrated *in vacuo*, leaving a thick brown oil that consisted of starting material and a mixture of monobenzylated and dibenzylated products (TLC monitoring, SiO_2, eluent CH_2Cl_2). Heating of the oily compound in water removed most of the starting naphthalene-based diol **1b**. Thereafter, the crude product was partitioned between H_2O and CH_2Cl_2, and the organic layer was separated and dried ($MgSO_4$). Filtration and concentration followed by FCC of the residue (silica gel, eluent $CHCl_3$) afforded **5a** (16.8 g, 33%), R_f = 0.71, as a side product, a slightly yellow thick oil, that solidified on standing: mp 57−58 °C (hexane−EtOH); ^{1}H NMR (300 MHz, $CDCl_3$) δ 5.20 (s, 2H), 5.25 (s, 2H), 6.79 (t, 1H, J = 5 Hz), 7.22−7.29 (m, 2H), 7.35−7.50 (m, 10H), 7.55 (t, 2H, J = 9 Hz), 8.32 (d, 1H, J = 9 Hz); ^{13}C NMR (75 MHz, $CDCl_3$) δ 70.1, 70.2, 103.7, 107.3, 118.1, 119.7, 124.2, 126.8, 127.5, 127.7, 128.0, 128.1, 128.7, 128.7, 121.3, 136.1, 137.1, 137.4, 154.9, 157.5; EIMS *m/z* (rel intens) 340 (64) $[M]^+$, 250 (48), 202 (11), 160 (48), 131 (37), 115 (16), 91 (100), 77 (30), 65 (64), 51 (43); HREIMS calcd for $C_{24}H_{20}O_2$ $[M]^+$ *m/z* 340.1463, found *m/z* 340.1468. A second fraction, after recrystallization from EtOAc−hexane, gave **5b** (1.2 g, 3%), R_f = 0.26 (exposure of the TLC plate to I_2 vapor gave a brown spot): mp 117−118 °C; ^{1}H NMR (300 MHz, $CDCl_3$) δ 5.17 (s, 2H), 5.33 (bs, 1H), 6.64 (dd, 1H, J = 7 Hz, J = 1 Hz), 7.18 (d, 1H, J = 2.5 Hz), 7.22 (dd, 1H, J = 9, 2.5 Hz), 7.24 (t, 1H, J = 7 Hz), 7.31 (d, 1H, J = 7 Hz), 7.34 (d, 1H, J = 7 Hz), 7.41 (t, 2H, J = 7 Hz), 7.48 (d, 2H, J = 7 Hz), 8.10 (d, 1H, J = 9 Hz); ^{13}C NMR (67.5 MHz, $CDCl_3$, 318 K) δ 70.2, 106.9, 107.5, 118.1, 119.7, 123.4, 126.7, 127.6, 128.0, 128.6, 119.9, 136.2, 137.0, 151.6, 157.4; EIMS *m/z* (rel intens) 250 (71) $[M]^+$, 160 (52), 131 (57), 115 (23), 102 (45), 91 (100), 77 (46), 65 (57), 51 (37), 39 (26). Anal. Calcd for $C_{17}H_{14}O_2$: C, 81.58, H, 5.64. Found: C, 81.33; H, 5.62. A third compound isolated from the column was identified as **5c** (6.4 g, 17%), R_f = 0.24 (exposure of the TLC plate to I_2 vapor gave a yellow spot), as a viscous oil: ^{1}H NMR (300 MHz, $CDCl_3$) δ 5.24 (s, 2H), 5.31 (bs, 1H), 6.77 (dd, 1H, J = 7, 1 Hz), 7.09 (dd, 1H, J = 9, 2.5 Hz), 7.11 (d, 1H, J = 2.5 Hz), 7.29 (d, 1H, J = 7 Hz), 7.35 (t, 1H, J = 7 Hz), 7.39 (d, 1H, J = 7 Hz), 7.45 (t, 2H, J = 7 Hz), 7.55 (d, 2H, J = 7 Hz), 8.28 (d, 1H, J = 9 Hz); ^{13}C NMR (75 MHz, $CDCl_3$) δ 70.2, 103.5, 109.6, 116.9, 119.3, 124.5, 126.9, 127.5, 128.0, 128.7, 121.2, 136.1, 137.3, 154.0, 154.9. Anal. Calcd for $C_{17}H_{14}O_2$: C, 81.58, H, 5.64. Found: C, 81.21; H, 5.79. As the R_f values of monobenzylated products **5b** and **5c** are very close, a mixed, unresolved fraction of the both compounds was also obtained (7.0 g, 19%).

1,11-Bis[1-(benzyloxy)-6-naphthoxy]-3,6,9-trioxaundecane (6a). NaH (1.25 g, 60% suspension in mineral oil, 0.031 mol) was added to a stirred solution of **5c** (6.3 g, 0.025 mol) in dry DMF (70 mL). After effervescence had subsided, the solution was heated to 80 °C, and on cessation of hydrogen evolution, a solution of tetraethylene glycol bistosylate (6.5 g, 0.013 mol) in dry DMF (50 mL) was added dropwise over 1 h. Stirring and heating were continued for 2 days. The reaction mixture was cooled to room temperature, the excess NaH was quenched with a few drops of H_2O, DMF was distilled off at low pressure, and the residue was partitioned between $CHCl_3$ and H_2O. The organic phase was washed with brine and dried ($MgSO_4$). Filtration and evaporation of the solvent afforded the crude product, which was subjected to FCC (SiO_2, 1−2% MeOH in CH_2Cl_2) to give **6a** (4.7 g, 57.1%) as a yellow thick oil: ^{1}H NMR (300 MHz, $CDCl_3$) δ 3.73 (m, 8H), 3.90 (t, 4H, J = 5 Hz), 4.22 (t, 4H, J = 5 Hz), 5.21 (s, 4H), 6.74 (dd, 2H, J = 6, 2 Hz), 7.09 (d, 2H, J = 2.5 Hz), 7.14 (dd, 2H, J = 9, 2.5 Hz), 7.30 (d, 2H, J = 6 Hz), 7.31 (d, 2H, J = 2 Hz), 7.35 (d, 2H, J = 7 Hz), 7.41 (t, 4H, J = 7 Hz), 7.51 (d, 4H, J = 7 Hz), 8.23 (d, 2H, J = 9 Hz); ^{13}C NMR (75 MHz, $CDCl_3$) δ 67.5, 69.8, 70.1, 70.8, 71.0, 103.5, 106.8, 118.0, 119.6, 124.0, 126.7, 127.5, 128.0, 128.6, 121.1, 136.0, 137.3, 154.8, 157.4; LSIMS *m/z* 658 $[M]^+$. Anal. Calcd for $C_{42}H_{42}O_7$: C, 76.57; H, 6.43. Found: C, 76.88; H, 6.65.

1,11-Bis(1-hydroxy-6-naphthoxy)-3,6,9-trioxaundecane (6b). A solution of the benzyl ether **6a** (4.4 g, 6.7 mmol) in CH_2Cl_2−MeOH (1:1, v/v, 80 mL) was subjected to hydrogenolysis over 10% Pd on charcoal (0.5 g) at atmospheric pressure. The catalyst was removed by flitration through Celite, and the solvent was evaporated to give **6b** (2.8 g, 87%) as colorless thick oil that solidified upon standing, mp 92−93 °C. The product was used in the next step without further purification: ^{1}H NMR (300 MHz, CD_3COCD_3) δ 3.66 (m, 8H), 3.86 (m, 4H), 4.21 (m, 4H), 6.77 (dd, 2H, J = 6, 2 Hz), 7.11 (dd, 2H, J = 9, 2.5 Hz), 7.20 (d, 2H, J = 2.5 Hz), 7.23 (d, 2H, J = 6 Hz), 7.25 (d, 2H, J = 2 Hz), 8.15 (d, 2H, J = 9 Hz), 9.05 (s, 2H); ^{13}C NMR (75 MHz, CD_3COCD_3) δ 68.2, 70.2, 71.2, 71.4, 107.0, 107.4, 118.0, 119.0, 124.5, 127.7, 121.1, 137.3, 154.1, 158.1; EIMS *m/z* (rel intens) 478 (41) $[M]^+$, 476 (63) $[M - 2]^+$, 318 (13), 271 (9), 231 (11), 204 (12), 187 (74), 160 (100), 131 (59), 115 (80).

1,6-Dinaphtho-36-crown-10 (4e). A solution of tetraethylene glycol bistosylate (2.6 g, 5.2 mmol) in dry MeCN (75 ml) and a solution of **6b** (2.5 g, 5.2 mmol) in dry MeCN (75 mL) were added simutaneously under nitrogen atmosphere over a period of 1 h to a stirred suspension of Cs_2CO_3 (8.5 g, 26.0 mmol) in MeCN (200 mL) heated under reflux. The reaction mixture was then heated at reflux for a further 3 days. After cooling, the reaction mixture was filtered through Celite, the solid was washed with MeCN and CH_2Cl_2, and the combined filtrate was concentrated *in vacuo*. The residue was partitioned between H_2O and CH_2Cl_2, and the organic layer was separated and dried ($MgSO_4$). After removal of the solvent, the crude product was purified by FCC (SiO_2, 2% MeOH in CH_2Cl_2) to afford **4e** (0.8 g, 24%), as a thick oil, that solidified on standing to give a white solid: mp 111−112 °C; ^{1}H NMR (300 MHz, CD_3COCD_3) δ 3.59−3.69 (m, 12 H), 3.71 (m, 4H), 3.84 (m, 4H), 3.93 (m, 4H), 4.15 (m, 4H), 4.21 (m, 4H), 6.73 (dd, 2H, J = 5, 1.5 Hz), 7.09 (dd, 2H, J = 9, 2.5 Hz), 7.17 (d, 2H, J = 2.5 Hz), 7.29 (d, 2H, J = 6 Hz), 7.30 (d, 2H, J = 2 Hz), 8.13 (d, 2H, J = 9 Hz); ^{13}C NMR (75 MHz, $CDCl_3$) δ 67.5, 68.0, 69.7, 69.8, 70.9, 71.0, 71.1, 103.1, 106.8, 117.8, 119.4, 123.9, 126.5, 121.0, 135.9, 154.8, 157.3; LSIMS *m/z* 636 $[M]^+$. Anal. Calcd for $C_{36}H_{44}O_{10}$: C, 67.91; H, 6.97. Found: C, 67.60; H, 7.03.

General Procedure for the Synthesis of [2]Catenanes 9a−k. Method A. 1,4-Bis(bromomethyl)benzene (231 mg, 0.88 mmol), the bis(hexafluorophospahte) **8**·2PF_6 (494 mg, 0.70 mmol), and the macrocyclic polyether (**4a**−**e**, **4h**−**k**) (0.35 mmol) were dissolved in dry DMF (15 mL). After the mixture was stirred at room temperature for 10 days, the solvent was removed *in vacuo* and the residue purified by column chromatography on silica gel (40 g, 230−400 mesh) using MeOH−2 M NH_4Cl−$MeNO_2$ (7:2:1) as eluent. The fractions containing the product were combined, and the solvent was evaporated *in vacuo*. The residue was dissolved in H_2O, and a saturated aqueous solution of NH_4PF_6 was added until no further precipitation was observed. The red solid was filtered off, washed with H_2O, and dried (60 °C/0.1 Torr) to yield the corresponding [2]catenane **9**, which was further purified by crystallization (MeCN/*i*-Pr_2O).

[2]Catenane 9a·4PF_6: yield 82%; mp > 250 °C; ^{1}H NMR (400 MHz, CD_3CN, 298 K) δ 3.37 (bs, 4H), 3.47 (m, 2H), 3.54 (m, 2H), 3.64−3.97 (m, 26H), 4.07 (bs, 2H), 5.62, 5.65, 5.67, 5.70 (AB system, 8H), 6.37 (bs, 1H), 6.67 (d, 1H, J = 8 Hz), 7.22 (bs, 1H), 7.32 (bs, 1H), 7.33 (bs, 2H), 7.47 (bs, 8H), 7.75 (s, 8H), 8.75 (d, 8H, J = 6.5 Hz); ^{13}C NMR (100.6 MHz, CD_3CN,

inverse $^{13}C-^{1}H$ correlation) δ 65.5, 67.5, 69.3, 69.4, 70.6, 70.8, 70.9, 71.0, 71.6, 71.6, 71.8, 72.2, 105.0, 109.1, 113.8, 118.5, 126.1, 128.4, 131.7, 145.3, 137.5, 146.5; LSIMS *m*/*z* 1541 [M − PF_6]$^+$, 1396 [M − $2PF_6$]$^+$, 1251 [M − $3PF_6$]$^+$; HRLSIMS *m*/*z* calcd for $C_{68}H_{74}N_4O_{10}F_3P_{18}$ [M − PF_6]$^+$ *m*/*z* 1541.4330, found *m*/*z* 1541.4431. Single crystals, suitable for X-ray crystallography, were grown by vapor diffusion of *i*-Pr_2O into a solution of **9a**·$4PF_6$ in MeCN.

[2]Catenane 9b·4PF$_6$: yield 89%; mp > 300 °C; ^{1}H NMR (400 MHz, CD_3SOCD_3, 300 K) δ 3.20 (s, 4H), 3.51 (m, 4H), 3.78−3.83 (m, 20H), 3.89 (s, 8H), 5.73 (s, 8H), 6.57 (bs, 2H), 6.73 (bd, 2H, *J* = 7.5 Hz), 7.19 (bd, 2H, *J* = 6.5 Hz), 7.88 (s, 8H), 7.92 (d, 8H, *J* = 5.5 Hz), 9.04 (d, 8H, *J* = 6 Hz); ^{13}C NMR (100.6 MHz, CD_3SOCD_3, 298 K, inverse $^{13}C-^{1}H$ correlation) δ 63.7, 65.9, 67.7, 68.9, 69.6, 69.9, 70.1, 70.3, 70.7, 106.6, 112.3, 118.7, 125.3, 128.2, 130.7, 144.1, 130.0, 137.0, 145.4, 149.6, 154.5; LSIMS *m*/*z* 1686 [M]$^+$, 1541 [M − PF_6]$^+$, 1396 [M − $2PF_6$]$^+$, 1251 [M − $3PF_6$]$^+$; HRLSIMS calcd for $C_{68}H_{74}N_4O_{10}F_3P_{18}$ [M − PF_6]$^+$ *m*/*z* 1541.4330, found *m*/*z* 1541.4269. Single crystals, suitable for X-ray crystallography, were grown by vapor diffusion of *i*-Pr_2O into a solution of **9b**·$4PF_6$ in MeCN−CH_3NO_2 (1:1, v/v).[17]

[2]Catenane 9c·4PF$_6$: yield 74%; mp > 300 °C; ^{1}H NMR (400 MHz, CD_3COCD_3, 298 K) δ 3.45 (m, 4H), 3.62 (m, 4H), 3.64 (bs, 4H), 3.78 (m, 4H), 3.85 (m, 4H), 3.91 (m, 4H), 3.97−4.00 (m, 12H), 5.99 (bs, 8H), 6.25 (d, 2H, *J* = 2 Hz), 6.93 (dd, 2H, *J* = 9.0, 2 Hz), 7.67 (d, 2H, *J* = 9 Hz), 7.86 (bs, 8H), 8.01 (s, 8H), 9.14 (bs, 8H); ^{13}C NMR (100.6 MHz, CD_3COCD_3, 298 K, inverse $^{13}C-^{1}H$ correlation) δ 65.6, 67.3, 68.5, 70.1, 70.6, 70.9, 71.7, 71.9, 106.1, 113.9, 117.0, 126.3, 130.7, 131.8, 145.5, 125.0, 136.7, 137.8, 147.0, 151.1, 158.0; LSIMS *m*/*z* 1686 [M]$^+$, 1541 [M − PF_6]$^+$, 1396 [M − $2PF_6$]$^+$, 1251 [M − $3PF_6$]$^+$; HRLSIMS calcd for $C_{68}H_{74}N_4O_{10}F_3P_{18}$ [M − PF_6]$^+$ *m*/*z* 1541.4330, found *m*/*z* 1541.4341. Anal. Calcd for $C_{68}H_{74}N_4O_{10}P_4F_{24}$: C, 48.41; H, 4.42; N, 3.32. Found: C, 48.56; H, 4.32; N, 3.52

[2]Catenane 9d·4PF$_6$: yield 51%, mp > 280 °C; ^{1}H NMR (400 MHz, CD_3CN, 313 K) δ 2.31 (d, 2H), 3.68−3.72 (bm, 4H), 3.76−3.79 (bm, 4H), 3.79−3.82 (bm, 4H), 3.89-3.94 (bm, 4H), 3.96−4.01 (bm, 4H), 4.02−4.06 (bm, 4H), 4.08−4.12 (bm, 4H), 4.21-4.24 (bm, 4H), 5.63 (d, 4H), 5.82 (t, 2H), 5.84 (d, 4H), 6.09 (d, 2H), 6.36 (d, 2H), 6.88 (bd, 8H), 7.12 (t, 2H), 7.18 (d, 2H), 7.88 (d, 4H), 8.04 (d, 4H), 8.39 (d, 4H), 8.86 (d, 4H); LSIMS *m*/*z* 1592 [M − PF_6]$^+$, 1446 [(M − 2 PF_6]$^+$, 1301 [M − 3 PF_6]$^+$.

[2]Catenane 9e·4PF$_6$. After counterion exchange with aqueous NH_4PF_6, the product was extracted into $MeNO_2$ and the organic phase was separated and washed with H_2O. The solvent was removed *in vacuo*, and the residue was dried (70 °C/0.1 Torr, 12 h) to give the [2]catenane **9e**·$4PF_6$. Yield: 35%, mp > 250 °C. ^{1}H NMR (400 MHz, CD_3CN, 238 K, 2D-COSY 45) δ 2.14 (d, 1H, *J* = 8.2 Hz), 2.48 (d, 1H, *J* = 9 Hz), 3.62−4.18 (m, 32H), 4.62 (d, 1H, *J* = 2 Hz), 5.17 (dd, 1H, *J* = 9 Hz, *J* = 2.5 Hz), 5.60, 5.63, 5.70, 5.73 (AB system, 8H), 5.77 (t, 1H, *J* = 8 Hz), 6.03 (d, 1H, *J* = 8 Hz), 6.20 (d, 1H, *J* = 7.5 Hz), 6.52 (d, 1H, *J* = 8 Hz), 6.68−6.74 (m, 3H), 6.89 (bs, 2H), 6.98 (bs, 2H), 7.04 (d, 2H, *J* = 4.7 Hz), 7.14 (d, 1H, *J* = 9 Hz), 7.27 (bs, 2H), 7.91 (m, 8H), 8.34 (d, 2H, *J* = 5.5 Hz), 8.49 (d, 2H, *J* = 5.5 Hz), 8.65 (d, 2H, *J* = 6.5 Hz), 8.90 (bs, 2H); ^{13}C NMR (75 MHz, CD_3CN) δ 65.8, 68.6, 69.1, 70.3, 70.4, 71.0, 71.1, 71.3, 104.5, 108.0, 126.0, 128.3, 128.4, 128.5, 130.2, 131.2, 131.8, 131.9, 145.2, 137.7, 145.9; LSIMS *m*/*z* 1737 [M + H]$^+$, 1591 [M − PF_6]$^+$, 1446 [M − $2PF_6$]$^+$, 1301 [M − $3PF_6$]$^+$; HRLSIMS calcd for $C_{72}H_{76}N_4O_{10}F_3P_{18}$ [M − PF_6]$^+$ *m*/*z* 1591.4487, found *m*/*z* 1591.4545. Single crystals, suitable for X-ray crystallography, were grown by vapor diffusion of *i*-Pr_2O into a solution of **9e**·$4PF_6$ in MeCN.

[2]Catenane 9h·4PF$_6$: yield 64%; mp > 250 °C; ^{1}H NMR (400 MHz, CD_3COCD_3, 298 K, 2D-COSY 45) δ 2.56 (d, 1H, *J* = 8.5 Hz), 2.62 (d, 1H, *J* = 8 Hz), 3.72 (s, 4H), 3.86 (s, 6H), 3.94 (m, 2H), 3.97 (m, 2H), 4.05−4.07 (m, 6H), 4.11 (s, 4H), 4.18 (m, 2H), 4.24 (m, 2H), 4.32 (m, 2H), 4.39 (m, 2H), 5.94−6.08 (m, 10H), 6.25 (d, 2H, *J* = 8 Hz), 6.32 (dd, 1H, *J* = 9, 2.5 Hz), 6.71 (d, 2H, *J* = 7.5 Hz), 7.06 (d, 1H, *J* = 8.5 Hz), 7.17 (d, 1H, *J* = 9 Hz), 7.23 (d, 1H, *J* = 8 Hz), 7.26 (m, 2H), 7.42 (m, 2H), 7.51 (m, 2H), 7.58 (d, 2H, *J* = 6.6 Hz), 8.12 (s, 2H), 8.18 (s, 2H), 8.31 (bs, 4H), 8.77 (m, 2H), 9.03 (d, 2H, *J* = 6.5 Hz), 9.17 (d, 2H, *J* = 7 Hz), 9.27 (d, 2H, *J* = 6.5 Hz); ^{13}C NMR (75 MHz, CD_3CN) δ 66.0, 69.0, 69.2, 69.7, 70.7, 70.9, 71.2, 71.9, 72.0, 72.2, 105.0, 105.2, 105.4, 109.3, 120.5, 124.3, 125.0, 125.3, 126.2, 128.6, 129.1, 130.7, 130.8, 131.4, 132.2, 144.6, 145.1, 120.9, 136.5, 137.6, 145.4, 152.0, 155.4, 157.9; LSIMS *m*/*z* 1737 [M + H]$^+$, 1591 [M − PF_6]$^+$, 1446 [M − $2PF_6$]$^+$, 1301 [M − $3PF_6$]$^+$; HRLSIMS calcd for $C_{72}H_{76}N_4O_{10}F_3P_{18}$ [M − PF_6]$^+$ *m*/*z* 1591.4487, found 1591.4552. Single crystals, suitable for X-ray crystallography, were grown by vapor diffusion of *i*-Pr_2O into a solution of **9h**·$4PF_6$ in MeCN.

[2]Catenane 9i·4PF$_6$: yield 74%; mp > 259 °C; ^{1}H NMR (400 MHz, CD_3CN, 303 K, 2D-COSY 45) δ 2.29, (d, 2H, *J* = 8.3 Hz), 3.67 (m, 4H), 3.72 (m, 4H), 3.79 (m, 4H), 3.83 (m, 4H), 3.94 (m, 4H), 4.12 (m, 4H), 4.09 (m, 4H), 4.15 (m, 4H), 5.60, 5.63, 5.80, 5.83 (AB system, 8H), 5.84 (t, 2H, *J* = 6 Hz), 6.10 (d, 2H, *J* = 7 Hz), 6.39 (d, 2H, *J* = 2 Hz), 6.70 (dd, 2H, *J* = 9, 2 Hz), 6.90 (d, 4H, *J* = 6 Hz), 6.96 (d, 4H, *J* = 6 Hz), 7.10 (d, 2H, *J* = 9 Hz), 7.85−8.08 (bm, 8H), 8.44 (d, 4H, *J* = 6.5 Hz), 8.72 (d, 4H, *J* = 7 Hz); ^{13}C NMR (75 MHz, CD_3CN) δ 65.8, 68.6, 69.0, 69.9, 70.6, 71.2, 72.2, 104.9, 107.5, 109.2, 119.8, 125.2, 126.2, 129.2, 132.0, 132.1, 144.5, 145.4, 131.1, 137.4, 145.1, 152.0, 155.9; LSIMS *m*/*z* 1736 [M]$^+$, 1591 [M − PF_6]$^+$, 1446 [M − $2PF_6$]$^+$, 1301 [M − $3PF_6$]$^+$; HRLSIMS calcd for $C_{72}H_{76}N_4O_{10}F_{12}P_2$ [M − $2PF_6$]$^+$ *m*/*z* 1446.4845, found *m*/*z* 1446.4801.

[2]Catenane 9j·4PF$_6$: yield 84%; mp > 250 °C; ^{1}H NMR (400 MHz, CD_3COCD_3, 303 K, 2D-COSY 45) δ 2.62 (d, 2H, *J* = 8 Hz), 3.47 (m, 4H), 3.75 (m, 4H), 3.88 (m, 4H), 3.96 (m, 4H), 4.03 (m, 4H), 4.08 (m, 4H), 4.20 (m, 4H), 4.32 (m, 4H), 5.98, 6.02, 6.09, 6.12 (AB system, 8H), 6.08 (t, 2H, *J* = 8 Hz), 6.12 (d, 2H, *J* = 3 Hz), 6.26 (d, 2H, *J* = 8 Hz), 6.86 (dd, 2H, *J* = 9, 2 Hz), 7.31 (bd, 4H), 7.37 (bd, 4H), 7.60 (d, 2H, *J* = 9 Hz), 8.15 (s, 4H), 8.35 (s, 4H), 8.91 (d, 4H, *J* = 6.0 Hz), 9.17 (d, 4H, *J* = 7 Hz); ^{13}C NMR (75 MHz, CD_3CN) δ 65.9, 68.6, 69.0, 70.0, 70.7, 71.2, 71.5, 72.3, 105.1, 106.1, 109.1, 117.0, 125.1, 126.1, 128.5, 129.2, 130.8, 131.3, 132.1, 144.6, 145.5, 118.3, 124.8, 125.2, 136.4, 137.5, 145.3, 151.9, 157.9; LSIMS *m*/*z* 1737 [M + H]$^+$, 1591 [M − PF_6]$^+$, 1446 [M − $2PF_6$]$^+$, 1301 [M − $3PF_6$]$^+$; HRLSIMS calcd for $C_{72}H_{76}N_4O_{10}F_3P_{18}$ [M − PF_6]$^+$ *m*/*z* 1591.4587, found 1591.4416. Single crystals, suitable for X-ray crystallography, were grown by vapor diffusion of *i*-Pr_2O into a solution of **9j**·$4PF_6$ in MeCN.

[2]Catenane 9k·4PF$_6$: yield 25%; mp > 250 °C; ^{1}H NMR (400 MHz, CD_3COCD_3, 273 K, 2D-COSY 45) δ 3.40 (s, 2H), 3.52 (s, 4H), 3.73 (s, 4H), 3.81 (s, 4H), 3.88 (m, 8H), 3.93 (s, 4H), 3.99 (s, 4H), 4.03 (s, 4H), 4.92 (d, 2H, *J* = 9 Hz), 5.98 (bs, 4H), 6.04 (bs, 4H), 6.32 (d, 4H, *J* = 6.5 Hz), 6.74 (d, 2H, *J* = 9 Hz), 7.29 (d, 2H, *J* = 9 Hz), 7.62 (bs, 4H), 7.80 (bs, 4H), 8.20 (s, 8H), 9.20 (s, 8H); ^{13}C NMR (75 MHz, CD_3CN) δ 65.7, 68.4, 70.5, 70.6, 71.1, 71.3, 71.5, 106.5, 107.7, 126.4, 128.1, 128.4, 128.5, 128.6, 130.1, 130.4, 130.4, 132.1, 145.3, 135.3, 138.1, 146.5, 155.1, 158.0; LSIMS *m*/*z* 1591 [M − PF_6]$^+$, 1446 [M − $2PF_6$]$^+$, 1301 [M − $3PF_6$]$^+$; HRLSIMS calcd for $C_{72}H_{76}N_4O_{10}F_3P_{18}$ [M − PF_6]$^+$ *m*/*z* 1591.4487, found *m*/*z* 1591.4522.

Method B. 1,4-Bis(bromomethyl)benzene (106 mg, 0.40 mmol), the bis(hexafluorophosphate) salt **8**·$2PF_6$ (226 mg, 0.32 mmol), and the macrocyclic polyether (102 mg, 0.16 mmol) were dissolved in hot, dry DMF (10 mL). The yellow solution was transferred to an ultrahigh-pressure reaction Teflon vessel, which was then compressed (12 kbar) at 40 °C for 5 days. After decompression of the reaction vessel, the orange-red reaction mixture was concentrated *in vacuo*. The solid residue was dissolved in a minimum amount of mixture $MeNO_2$−MeOH (1:1) and subjected to column chromatography (MeOH/2M NH_4Cl/$MeNO_2$, 7:2:1) on silica gel (65 g, 230−400 mesh), and fractions containing the catenane were combined. Removal of the solvent *in vacuo*, followed by counterion exchange, afforded an orange precipitate that was filtered off, washed with water, and dried (60 °C/0.1 Torr).

[2]Catenane 9g·4PF$_6$: yield 27%; mp > 300 °C; ^{1}H NMR (400 MHz, CD_3CN, 233 K) δ 3.36 (bs, 2H), 3.64−3.87 (m, 32H),

(17) The author has deposited atomic coordinates for this structure with the Cambridge Crystallographic Data Centre. The coordinates can be obtained, on request, from the Director, Cambridge Crystallographic Data Centre, 12 Union Road, Cambridge, CB2 1EZ, UK.

4.28 (d, 2H, J = 8 Hz), 5.62 (s, 4H), 5.68 (s, 4H), 5.81 (dd, 2H, J = 9, 2 Hz), 6.48 (dd, 2H, J = 9, 2 Hz), 6.57 (d, 2H, J = 2 Hz), 6.82 (d, 2H, J = 9 Hz), 7.10 (bd, 4H), 7.13 (bd, 4H), 7.88 (s, 8H), 8.63 (d, 4H, J = 6 Hz), 8.70 (d, 4H, J = 5 Hz); ^{13}C NMR (75 MHz, CD_3CN) δ 65.6, 68.2, 70.3, 71.2, 106.3, 126.4, 129.1, 131.4, 132.0, 145.4, 138.2, 146.8, 157.6; LSIMS m/z 1591 [M − PF_6]$^+$, 1446 [M − $2PF_6$]$^+$, 1301 [M − $3PF_6$]$^+$; HRLSIMS calcd for $C_{72}H_{76}N_4O_{10}F_3P_{18}$ [M − PF_6]$^+$ m/z 1591.4508, found m/z 1591.4487.

[2]Catenane 9f·4PF$_6$: yield 16%; mp > 250 °C; ^{1}H NMR (400 MHz, CD_3COCD_3, 273 K) δ 3.36 (s, 2H), 3.80 (m, 12H), 3.89 (m, 8H), 3.92 (m, 4H), 3.99 (m, 4H), 4.06 (m, 4H), 4.95 (d, 2H, J = 9 Hz), 6.03 (bs, 8H), 6.31 (dd, 2H, J = 8, 2 Hz), 6.58 (s, 2H), 6.66 (dd, 2H, J = 9, 2 Hz), 7.07 (d, 2H, J = 9 Hz), 7.72 (bs, 8H), 8.22 (s, 8H), 9.21 (d, 8H, J = 6.8 Hz); ^{13}C NMR (75 MHz, CD_3COCD_3) δ 65.7, 68.1, 70.4, 71.0, 126.2, 128.2, 128.3, 130.1, 131.3, 132.3, 145.3, 138.3, 146.4; LSIMS m/z 1591 [M − PF_6]$^+$, 1446 [M − $2PF_6$]$^+$, 1301 [M − $3PF_6$]$^+$; HRLSIMS calcd for $C_{72}H_{76}N_4O_{10}F_3P_{18}$ [M − PF_6]$^+$ m/z 1591.4487, found m/z 1591.4487.

Determination of the Association Constants by UV−vis and ^{1}H-NMR Spectroscopy. Method A. The association constants for the 1:1 complexes incorporating the π-electron-rich macrocycles **4a**−**k** and the bis(hexafluorophosphate) salt of paraquat [**PQT**]·$2PF_6$ were determined by UV−vis spectroscopy, employing the titration methodology.[9] A series of solutions, having a fixed concetration (~10^{-3} M) of the π-electron-rich macrocyle **4a**−**k** and containing different amounts of [**PQT**]·$2PF_6$ (from ~10^{-4} to 10^{-2} M) in Me_2CO, were prepared. The absorbances at the wavelength (λ_{max}) corresponding to the maxima of the charge transfer bands of the appropriate 1:1 complexes were measured for all the solutions. The correlations between the absorbances and the guest concentrations were used to evaluate the association constants (K_a) using a nonlinear curve-fitting program.

Method B. The association constants for the 1:1 complexes incorporating the π-electron-rich guests **2a**−**e** and the tetracationic cyclophane **10**·$4PF_6$ were determined by ^{1}H NMR spectroscopy employing the continuous variations methodology.[9] A solution of the teracationic cyclophane **10**·$4PF_6$ and solutions of the π-electron-rich acyclic guests **2a**−**e** having the same concentration (~10^{-3}) were prepared using CD_3CN as the solvent. By employing the two stock solutions, a range of solutions, having the same total volumes but differing in the ratio of the two components (from 1:9 to 9:1, host:guest), were prepared. The chemical shifts of the protons attached to the bipyridinium units of the host were measured by ^{1}H NMR spectroscopy at 25 °C. The correlations between the molar fractions of the hosts and the chemical shift changes for the probe protons were used to evaluate the association constants (K_a) using a nonlinear curve-fitting program.

X-ray Crystallography. Data were collected with graphite-monochromated Cu−Kα radiation using ω-scans. Lattice parameters were determined by least-squares fits from 18 to 22 centered reflections. Intensities were corrected for the decay of three control reflections measured every 97 reflections and for Lorentz and polarization factors, but not for absorption. The structures were solved by direct methods and refined by full or block matrix least-squares methods. Reflections with [$|F_o| > 4\sigma(|F_o|)$] were considered to be observed and were included in the refinements (based on F_o for **9b** and F_o^2 for the other [2]catenanes). All hydrogen atoms, where calculable, were included in the refinements in calculated positions and allowed to ride on their parent carbon atoms [$U(H) = 1.2U_{eq}(C)$, $U(H) = 1.5\ U_{eq}(CMe)$]. Parameters refined were the overall scale factor, isotropic extinction parameter, and positional parameter for the non-hydrogen atoms. There is disorder in some of the hexafluorophosphate counterions in the cases of all the [2]catenanes with the exception of **9b**. In all cases, two partial occupancy orientations were identified. All the structures contain disordered partial occupancy solvent molecules, with the exception of **9b** and **9h**. There is disorder in one of the polyether chains of **9a**, **9h**, and **9j**.

Electrochemistry. Cyclic voltammograms were recorded and analyzed at room temperature. Experiments were performed in deareated acetonitrile solutions under a nitrogen atmosphere. Analyte concentrations were held constant in the 0.1−0.5 mM range. Measurements were conducted in a standard single compartment cell. Tetrabutylammonium hexafluorophosphate (0.1 M) was used as the supporting electrolyte. A glassy carbon electrode (28 mm^2) was used as the working electrode; its surface was routinely polished with a 0.5 μm alumina slurry on a felt suface immediately prior to use. All potentials were recorded against an standard calomel electrode, and a platinum coil was used as the counter electrode. The cell potential was cycled from 0 to −1.2V (vs SCE) for all samples.

Acknowledgment. This research was supported by the Engineering and Physical Sciences Research Council and by the European Community Human Capital and Mobility Programme.

Supporting Information Available: Variable-temperature ^{1}H-NMR chemical shift data and derived free energy barriers associated with the dynamic processes occurring within the [2]catenanes **9a**−**k**·$4PF_6$ in solution (17 pages). This material is contained in libraries on microfiche, immediately follows this article in the microfilm version of the journal, and can be ordered from the ACS; see any current masthead page for ordering information.

JO961025C